

Supporting Information

for

Adaptable 2,5-bis((1,2,3-triazol-4-yl)methoxy)pyrazine ligands for the simple self-assembly of homoleptic 1D coordination polymers

Marryllyn E. Donaldson,^a Tyson N. Dais,^a Gareth J. Rowlands,^{ab} Brodie E. Matheson,^a and Paul G. Plieger^{*b}

^a*School of Natural Sciences (SNS), Massey University, Tennent Drive, Palmerston North, 4410, New Zealand*

E-mail: p.g.plieger@massey.ac.nz

Table of Contents

S1: Materials and Methods	2
<i>S1.1 Synthesis and characterisation of the azido derivatives</i>	3
<i>S1.3 Synthesis and characterisation of the TzOP ligands</i>	9
<i>S1.4 SCXRD of organic compounds</i>	12
S2 Characterization of Products	13
<i>S2.1 UV-Vis Spectroscopy</i>	13
<i>S2.2 L1 and L2 complexes</i>	14
<i>S2.3 L3complexes</i>	19
<i>S2.4 L3complexes</i>	20
S3 NMR Spectra	23
S4 Infrared Spectra	31
References	40

Experimental section

S1: Materials and Methods

Materials

All reactions were performed under aerobic conditions using chemicals and solvents as purchased from commercial sources, unless stated otherwise. MeOH was dried over activated 3 Å molecular sieves. **CAUTION:** Organic azides are potentially explosive and should be handled with care.

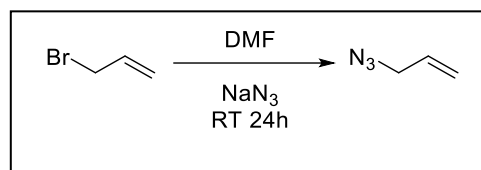
Instrumentation

- ^1H NMR and ^{13}C NMR spectra were recorded using a Bruker Avance 500 MHz spectrometer. Shifts are reported relative to residual solvent.
- IR spectra were recorded on solid-state samples using a ThermoFischer Nicolet iS5 equipped with an iD7 diamond ATR sampling accessory.
- HRMS was recorded using a ThermoScientific Q Exactive Focus Hybrid Quadrupole-Orbitrap mass spectrometer.
- UV-Vis spectra were recorded using a Shimadzu UV-3101PC spectrophotometer.
- Single-crystal X-ray diffraction experiments were carried out on a Bruker D8 Venture diffractometer equipped with an I μ S Diamond microfocus Cu-K α source ($\lambda = 1.54178 \text{ \AA}$) and a Photon III detector. Single crystals were mounted on MiTeGen mylar loops using Fomblin Y® and cooled to 100 K with an Oxford Cryostream 800. CCDC deposition numbers: 2301236-2301247

S1.1 Synthesis and characterisation of the azido derivatives

a1: Allyl azide¹

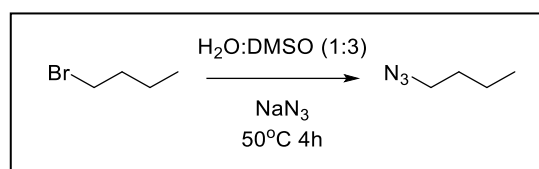
3-Bromo-1-propene (0.790 mL, 8.89 mmol, 1 equiv.) was added to a stirred suspension of sodium azide (0.7437 g, 11.44 mmol, 1.29 equiv.) in DMF (6 mL). After stirring at RT for 1 day, 10 ml of H₂O was added to the solution, and the product was extracted with CH₂Cl₂ (15 mL x3). The combined organic phases were concentrated to approximately half the original volume under reduced pressure (maintaining a temperature below 10 °C). The crude product was obtained within solution a in 42% yield (calculated from ¹H NMR) and was used without further purification.



¹H NMR (400 MHz, CDCl₃): δ 5.80-5.87 (ddt, 1H, *J*-1 = 16.44; *J*-2 = 10.30; *J*-3 = 6.24 Hz), 5.27 (m, 2H), 3.75 (d, 2H, *J* = 5.39 Hz) ppm.

a2: Azidobutane²

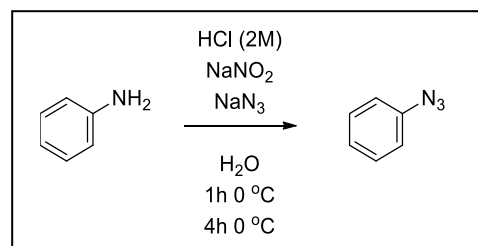
DMSO (6 mL) was added to a stirred solution of sodium azide (0.7116 g, 10.95 mmol, 1.5 equiv.) in water (2 mL) at RT. 1-Bromopropane (0.789 mL, 7.30 mmol, 1 equiv.) was then added. The mixture was stirred at 50 °C for 4 hours, after which two layers formed. The top layer contained the crude product as a clear oil, and was decanted for use in subsequent click reactions. The crude product was obtained in 97% yield (0.44 g). Analytical data is consistent with the literature.



¹H NMR (400 MHz, CDCl₃): δ 3.26 (t, 2H, *J* = 6.95 Hz), 1.56-1.62 (pent, 2H, *J* = 14.69; 7.24; 7.24 Hz), 1.37-1.47 (sext, 2H, *J*-1 = 22.40; *J*-2 = 7.39; *J*-3 = 7.39 Hz), 0.92-0.96 (t, 3H, *J* = 7.37 Hz) ppm. Mass (m/z): 122.05 (100), 123.05 (5) [M+Na]

a3: Phenyl azide³

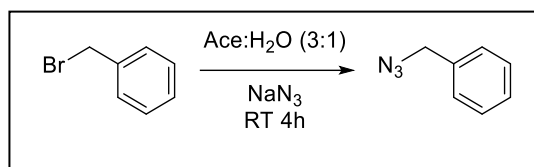
A solution of NaNO₂ (0.2908 g, 4.2 mmol, 1.11 equiv.) in water (6 mL) was added dropwise to a stirred solution of aniline (0.35 g, 3.8 mmol, 1 equiv.) in HCl (2 M, 11 mL) cooled in an ice bath. The reaction mixture was allowed to stir for one hour, after which sodium azide (0.6850 g, 10 mmol, 2.8 equiv.) dissolved in 12 mL water was added dropwise. The reaction was stirred for a further 4 hours at RT. The mixture was extracted with ethyl acetate (30 mL x3) and the combined organic extracts were washed with H₂O, dried over anhydrous Na₂SO₄, filtered, and concentrated under reduced pressure to give **a3** as a transparent yellow oil (0.3559 g, 88.49 %). The crude product was used directly without purification.



¹H NMR (CDCl₃, 500 MHz): δ 7.33-7.37 (t, 2H, *J* = 7.89 Hz), 7.12-7.15 (t, 1H, *J* = 7.42 Hz), 7.02-7.04 (d, 2H, *J* = 7.64 Hz) ppm. The analytical data are consistent with the literature.⁴

a4: Benzyl Azide⁵

Benzyl bromide (0.350 mL, 2.9 mmol, 1 equiv.) was added dropwise to a stirred solution of sodium azide (0.285 g, 4.4 mmol, 1.5 equiv.) in (3:1 acetone/water, 4 mL) at RT and allowed to react for 3 hours. The reaction was diluted with water and extracted with ethyl acetate (10 mL x3). The combined organic layers were washed with brine, dried over anhydrous MgSO₄, filtered, and concentrated under reduced pressure at 25 °C, to give crude benzyl azide as a transparent light-yellow oil in 95% yield (0.370 g). The product was used without further purification.

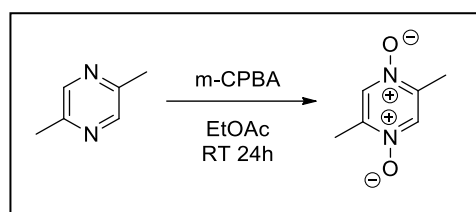


¹H NMR (CDCl₃, 500 MHz): δ = 7.31-7.41 (m, 5 H), 4.34 (s, 2 H) ppm. The analytical data are consistent with the literature.⁶

S1.2 Synthesis and characterisation of the alkyne derivative

1: 2,5-Dimethylpyrazine-1,4-N-oxide⁷

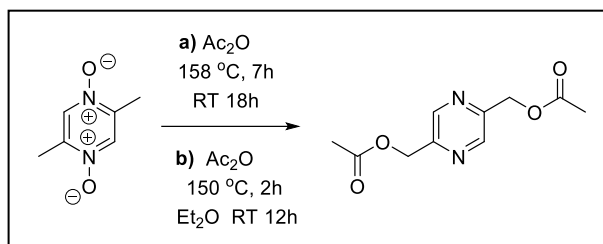
A solution of *m*-CPBA 77% (39.955 g, 178.28 mmol, 3 equiv.) in EtOAc (66 mL) was washed with brine (66 mL). The organic layer was separated, dried with MgSO₄, and filtered. 2,5-Dimethylpyrazine (6.5 mL, 59.428 mmol, 1 equiv.) was slowly added to the filtrate and the mixture was stirred for 24 hours at RT. The resulting white precipitate was collected over a glass frit, and washed with EtOAc (3x 15 mL), to remove any byproducts. The white solid, was dried to give **1** in an 87% yield (7.2660 g).



¹H NMR (500 MHz, DMSO-*d*₆): δ 8.48 (s, 1H), 2.23 (s, 3H) ppm.

2: 2,5-Bis(acetoxymethyl)pyrazine⁷

Method 1: A stirred suspension of **1** (5.001 g, 35.7 mmol, 1 equiv.) in acetic anhydride (25 mL, 260 mmol, 7.4 equiv.) was heated at 158 °C for 7 hours, then allowed to cool to RT and stirred for a further 16 hours. The acetic anhydride was



removed under reduced pressure to give a viscous black/brown liquid. Diethyl ether (125 mL) was added to the crude product, as an extraction solvent, and stirred vigorously for 2 hours, then stood for 3 hours at RT. The solution was then filtered through a thin pad of Celite, and the yellow filtrate collected. The solid crude residue was washed with additional 10 mL x4 until minimal colour was extracted with Et₂O. The combined filtrates were concentrated under reduced pressure. The product was washed with RT 3:7 EtOAc:Hexane, and the remaining dark orange product was hot recrystallised from 3:7 EtOAc:Hexane, affording **2** as a light yellow crystalline in 25% yield.

Optimisation of Method 2:

The low yield of this reaction was a bottleneck for ligand synthesis. To increase the reaction efficiency in both time and yield, an initial reaction of compound **1** with 7 equiv. of acetic anhydride at 100 °C for 1 hour indicated partial conversion to the desired product. A series of reactions lead to optimised conditions of compound **1** with 5 equiv. of acetic anhydride at 140 °C for 3 hours.

Method 2:

Acetic anhydride (1.87 mL, 19.5 mmol, 5 equiv.) was bubbled with Ar for one minute and added to a microwave vial containing 2,5-dimethylpyrazine (**1**) (0.55 g, 3.9 mmol, 1 equiv.) which was sealed, then heated under stirring to 140 °C for 3 hours using a microwave. The excess acetic anhydride was removed under reduced pressure. Diethyl ether (40 mL) was added to the black solid and stirred at RT for two hours. A black solid byproduct was removed by filtration, and the yellow filtrate was concentrated under reduced pressure. The resulting yellow solid was purified by hot recrystallisation with EtOAc:Hexane (1:3) (0.37 g, 47 %) affording **2** as yellow plate crystals in a 47% yield (0.37 g).

¹H NMR (500 MHz, CDCl₃): δ 8.61, (s, 2H), 5.25 (s, 2H), 2.15 (s, 3H) ppm. Mass (*m/z*): [M+H]: 225.13 (100), 226.10 (9) [M+Na]: 247.16 (100), 248.16 (11). These results agreed with literature values.

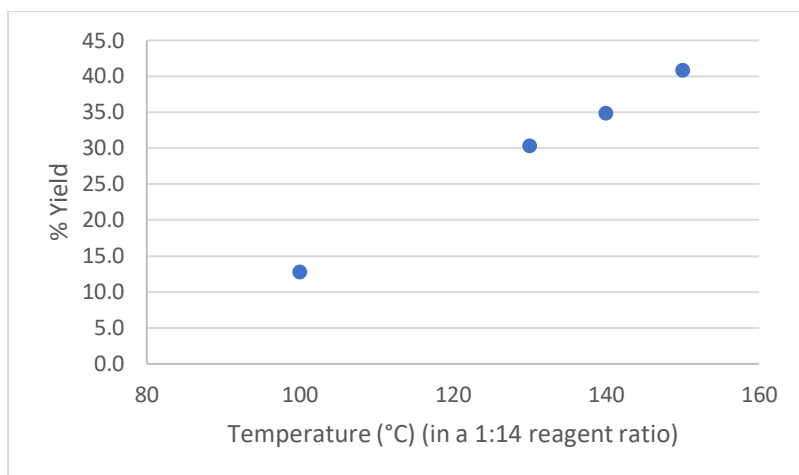


Figure S1 Product 2 yield: held at increasing temperature (a 1:14 1: Ac₂O ratio, held for one hour) yield increase

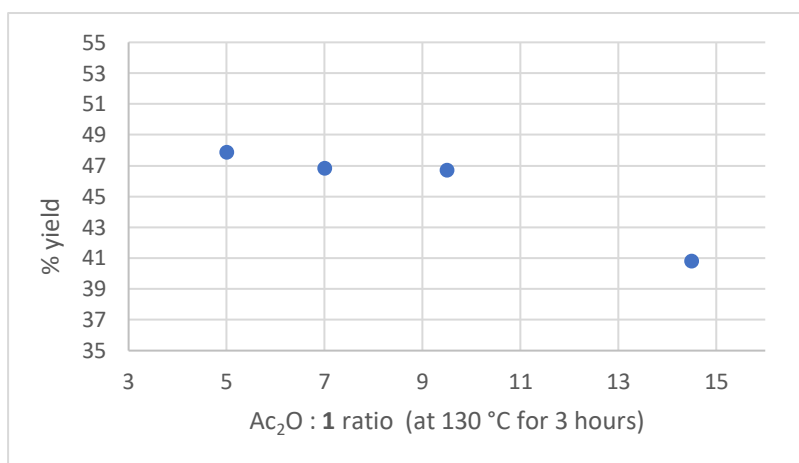


Figure S2 Product 2 yield: with variable Ac₂O to reagent 1 ratio (held at 130 °C for three hours). The optimal ratio was 5:1.

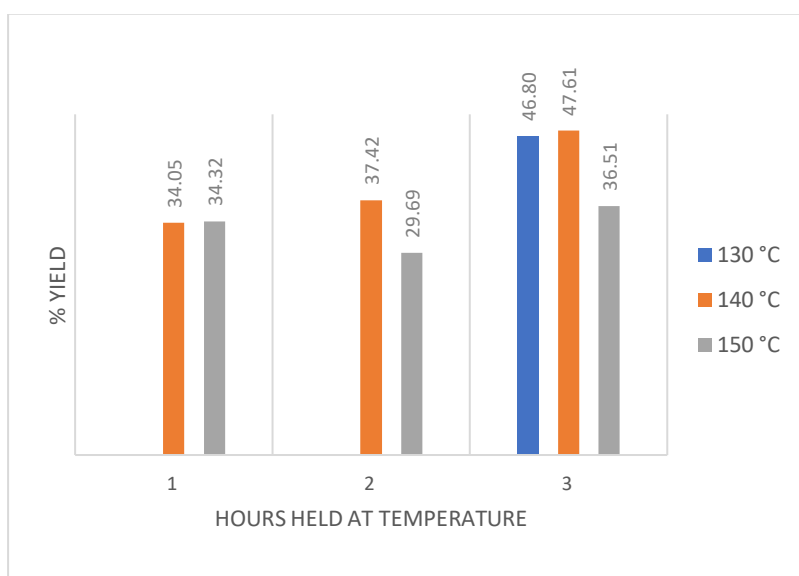


Figure S3 Product 2 yield: held at temperature for three hours (in a 5:1 ratio of Ac₂O:1).

X-ray crystal structure of **2**: 2,5-bis(acetoxymethyl)pyrazine

Yellow plate crystals suitable for single-crystal X-ray diffraction analysis were obtained from the addition of water into a methanolic solution of **2**. The data was solved and refined in the monoclinic space group $P2_1/c$, with the twin law $[-1, 0, 0, 0, -1, 0, 0, 0, 1]$ and BASF [0.450(6)]. The asymmetric unit contains half unit of the molecule with no additional solvent present.

Crystal Data for $C_{10}H_{12}N_2O_4$ ($M = 224.22$ g/mol): monoclinic, space group $P2_1/c$ (no. 14), $a = 11.3960(17)$ Å, $b = 5.4689(8)$ Å, $c = 8.3487(13)$ Å, $\beta = 90.197(9)^\circ$, $V = 520.32(14)$ Å³, $Z = 2$, $T = 100$ K, $\mu(\text{CuK}\alpha) = 0.949$ mm⁻¹, $\rho_{\text{calc}} = 1.431$ g cm⁻³, 5326 reflections measured ($7.758^\circ \leq 2\theta \leq 136.37^\circ$), 927 unique ($R_{\text{int}} = 0.0966$, $R_{\text{sigma}} = 0.0662$) which were used in all calculations. The final R_1 was 0.0780 ($I \geq 2\sigma(I)$) and wR_2 was 0.2152 (all data).

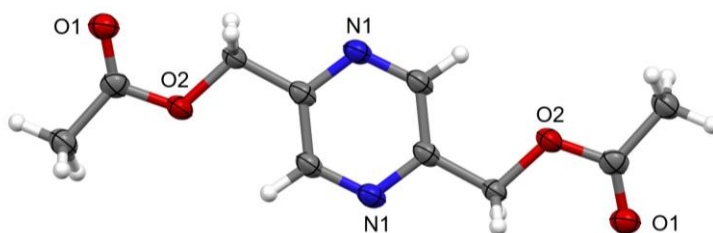
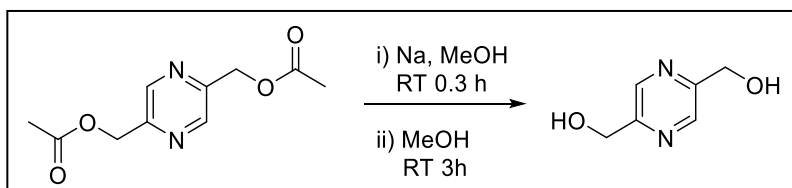


Figure S4 X-ray crystal structure showing a whole molecule of compound **2**, with labelled heteroatoms. Ellipsoids are drawn at the 50% probability level.

3: 2,5-Bis(hydroxymethyl)pyrazine⁷

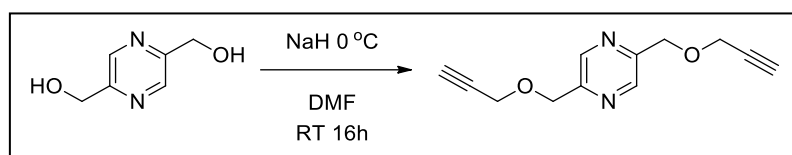


Fresh NaOMe solution was prepared by the piecewise addition of solid Na (0.3236 g, 14.1 mmol 2 equiv.) into dry MeOH (3 mL), followed by stirring for 15 minutes until no more solid remained.⁸

To the freshly prepared NaOMe was added a solution of **2** (1.5781 g, 7.04 mmol, 1 equiv.) in dry MeOH (35 mL) under argon, which was stirred for 3 hours at RT. The reaction was quenched by adding solid NH₄Cl (0.05 g). The solvent was concentrated under reduced pressure, resulting in the 2,5-bis(hydroxymethyl)pyrazine product as a beige-white solid, 0.9152g, in a 92.8%. This procedure resulted in the product **3**, that required no further purification, its characterisation agreeing with literature values.⁷

¹H NMR (500 MHz, CDCl₃): δ 8.57, (s, 1H, Ar-H), 4.84, (s, 2H, CH₂), 2.98 (br, 1H, -OH) ppm.

MS (*m/z*): [M+H] 141.17 (100), 142.11 (7) These results agreed with literature values.⁷



4: 2,5-Bis((prop-2-yn-1-yloxy)methyl)pyrazine

Adapted from Delso, *et al.*⁹ Compound **3** (0.743 g, 5.3 mmol, 1 equiv.) was ground with a mortar and pestle into a fine beige powder, that was suspended in 65 mL of DMF, bubbled with Ar, and cooled to 0°C. To this stirred solution, NaH (0.848 g, 21.2 mmol, 4 equiv.) was added in small portions. When hydrogen liberation stopped, propargyl bromide (0.95 mL, 10.75 mmol, 3 equiv.) was added dropwise. The reaction solution was stirred overnight at RT. The mixture was poured into 100 mL of ice water and the product extracted with hexane (3 x 100 mL). The combined organic layers were dried with MgSO₄, filtered and the solvent was removed under vacuum. Compound **4** was obtained as a clear, pale-yellow oil (0.713 g, 83%).

¹H NMR (500 MHz, DMSO-*d*₆): δ 8.63 (s, 2H), 4.68 (s, 4H), 4.30 (d, 4H, J = 2.44 Hz), 3.51 (t, 2H, J = 2.4 Hz) ppm. ¹³C NMR (126 MHz; DMSO-*d*₆): δ 152.21, 142.97, 80.31, 78.29, 70.29, 58.16 ppm.

IR: $\bar{\nu}_{\max}$ 2954, 2923, 2853, 1666, 1456, 1377, 1260, 736 cm⁻¹. HRMS (*m/z*) (ESI⁺): calculated for C₁₂H₁₃N₂O₂⁺ *m/z* = 217.0972 [L+H]⁺. Found (*m/z*): 217.0968 [L+H]⁺, 239.0787 [L+Na].

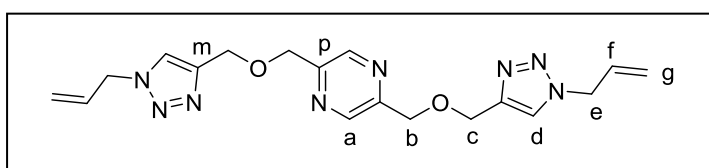
S1.3 Synthesis and characterisation of the TzOP ligands

General CuAAC click synthesis of L1-L4:

The pyrazine bis-alkyne compound, **4**, (1 equiv.) was reacted with the appropriate azide (2 equiv.) in a DCM:H₂O (10:1) solution. A catalytic amount (0.1 equiv.) of sodium ascorbate was added and stirred at RT for 5 min until dissolved. An aqueous solution of Cu(OAc)₂·6H₂O (0.1 equiv. 0.5M) was added to the reaction. After stirring overnight, the reaction was washed with H₂O until no further colour was removed. The organic solutions were also washed with 5 wt% EDTA aqueous solution followed by passage of the organic fraction through a silica plug and then concentrated under reduced pressure. The crude product was then dissolved in a minimal amount of MeOH, and the product crystallised upon the addition of water.

Ligand L1: 2,5-bis(((1-allyl-1H-1,2,3-triazol-4-yl)methoxy)methyl)pyrazine

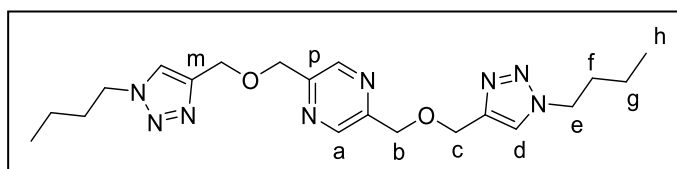
Following the general CuAAC method, using azido propene (**a1**) a light brown precipitate of **L1** was obtained in an 81% yield.



m.p. 90-97 °C. ¹H NMR (500 MHz, DMSO-d₆) δ: = 8.63 (s, 2H), 8.14 (s, 2H), 6.04 (ddt, 2H, *J*-1 = 6.29, *J*-2 = 10.38, *J*-3 = 5.26 Hz), 5.25 (d, 2H, *J* = 10.2 Hz), 5.15 (d, 2H, *J* = 16.94 Hz) 5.01 (d, 4H, *J* = 5.93 Hz), 4.68 (s, 8H) ppm. ¹³C NMR (126 MHz, DMSO-d₆) δ: = 152.5, 144.1, 142.8, 133.2, 124.7, 119.2, 70.8, 64.0, 52.1, 36.2, 31.2 ppm. **IR:** $\bar{\nu}_{\max}$ 3430, 3143, 2929, 1664, 1490, 1464, 1420, 1390, 1338, 1260, 1223, 1140, 1095, 1049, 1033, 993, 942, 886, 834, 793 cm⁻¹. **HRMS (*m/z*) (ESI+):** calculated for C₁₈H₂₃N₈O₂⁺ *m/z* = 383.1085 [M+H]⁺. Found *m/z* = 383.05 [M+H]; 405.12 [M+Na]; 787.28 [2M+Na].

L2: 2,5-Bis(((1-butyl-1H-1,2,3-triazol-4-yl)methoxy)methyl)pyrazine

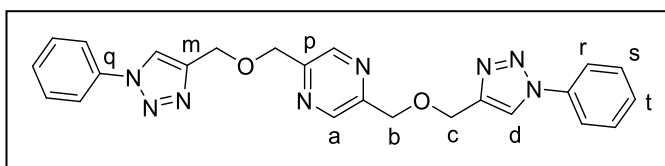
Following the general CuAAC method, using azido butane (**a2**) a white precipitate of **L2** was obtained in a 78% yield.



m.p. 89-96 °C. ¹H NMR (500 MHz, DMSO-d₆): δ 8.63 (2H, s), 8.17 (2H, s), 4.67 (4H, s), 4.66 (4H, s), 4.34 (4H, t, *J* = 7.05 Hz), 1.78 (4H, q, *J* = 7.33 Hz), 1.23 (4H, hex, *J* = 7.45), 0.88 (6H, t, *J* = 7.38 Hz) ppm. ¹³C NMR (126 MHz; DMSO-d₆): δ 152.5, 143.9, 142.8, 124.5, 70.7, 64.1, 49.5, 32.1, 19.5, 13.8 ppm **IR:** $\bar{\nu}_{\max}$ 3430, 3118, 2955, 2931, 2872, 1669, 1484, 1458, 1375, 1349, 1255, 1218, 1143, 1091, 1056, 1035, 1027, 991, 941, 870, 802, 776 cm⁻¹. **HRMS (*m/z*) (ESI+):** calculated for C₂₀H₃₁N₈O₂⁺ *m/z* = 415.2560 [M+H]⁺. Found *m/z* = 415.2564 [M+H]⁺, 437.2380 [L+Na]⁺

L3: 2,5-Bis(((1-phenyl-1H-1,2,3-triazol-4-yl)methoxy)methyl)pyrazine

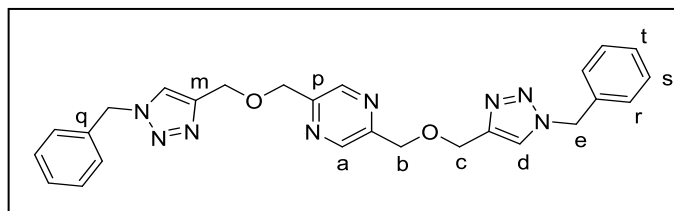
Following the general CuAAC method, using phenyl azide (**a3**), a pale orange-brown precipitate of **L3** was obtained in a 74% yield.



m.p. 177-184 °C. $^1\text{H NMR}$ (500 MHz, DMSO- d_6): δ 8.89 (s, 2H), 8.71 (s, 2H), 7.91 (d, 4H, $J = 8.31$ Hz), 7.60 (t, 4H, $J = 7.62$ Hz), 7.50 (t, 2H, $J = 7.35$ Hz), 4.78 (s, 4H), 4.76 (s, 4H) ppm. $^{13}\text{C NMR}$ (126 MHz; DMSO- d_6): δ 152.5, 145.2, 142.9, 137.1, 130.4, 129.1, 122.9, 120.5, 70.9, 63.9 ppm. **IR**: $\bar{\nu}_{\text{max}}$ 3400, 3125, 3078, 2920, 2860, 1598, 1557, 1501, 1480, 1466, 1445, 1386, 1345, 1264, 1236, 1196, 1095, 1053, 1030, 998, 944, 758, 689 cm^{-1} . **HRMS** (m/z) (**ESI+**): calculated for $\text{C}_{24}\text{H}_{24}\text{N}_8\text{O}_2^+$ $m/z = 455.1938$ [$\text{L}+\text{H}$] $^+$. Found (m/z): 455.1933 [$\text{L}+\text{H}$], 477.1752 [$\text{L}+\text{Na}$].

L4: 2,5-bis(((1-benzyl-1H-1,2,3-triazol-4-yl)methoxy)methyl)pyrazine

Following the general CuAAC method, using benzyl azide (**a4**), a pale brown precipitate of **L4** obtained in a 63% yield.



m.p. 125-129 °C. $^1\text{H NMR}$ (500 MHz, DMSO- d_6): δ 8.62 (s, 2H), 8.24 (s, 2H), 7.35-7.37 (m, 4H), 7.29-7.32 (m, 6H), 5.59 (s, 2H), 4.67 (s, 4H), 4.66 (s, 4H) ppm. $^{13}\text{C NMR}$ (126 MHz; DMSO- d_6): δ 152.5, 144.4, 142.8, 136.5, 129.2, 128.6, 128.4, 124.8, 70.8, 64.0, 53.2 ppm. **IR**: $\bar{\nu}_{\text{max}}$ 3408, 3130, 3065, 3031, 2925, 2096, 1605, 1497, 1455, 1435, 1362, 1333, 1217, 1157, 1123, 1076, 1053, 1030, 987, 824, 720, 696, 576 cm^{-1} . **HRMS** (m/z) (**ESI+**): calculated for $\text{C}_{26}\text{H}_{27}\text{N}_8\text{O}_2^+$ $m/z = 483.2251$ [$\text{L}+\text{H}$] $^+$. Found (m/z): 505.2065 [$\text{L}+\text{Na}$], 483.2247 [$\text{L}+\text{H}$].

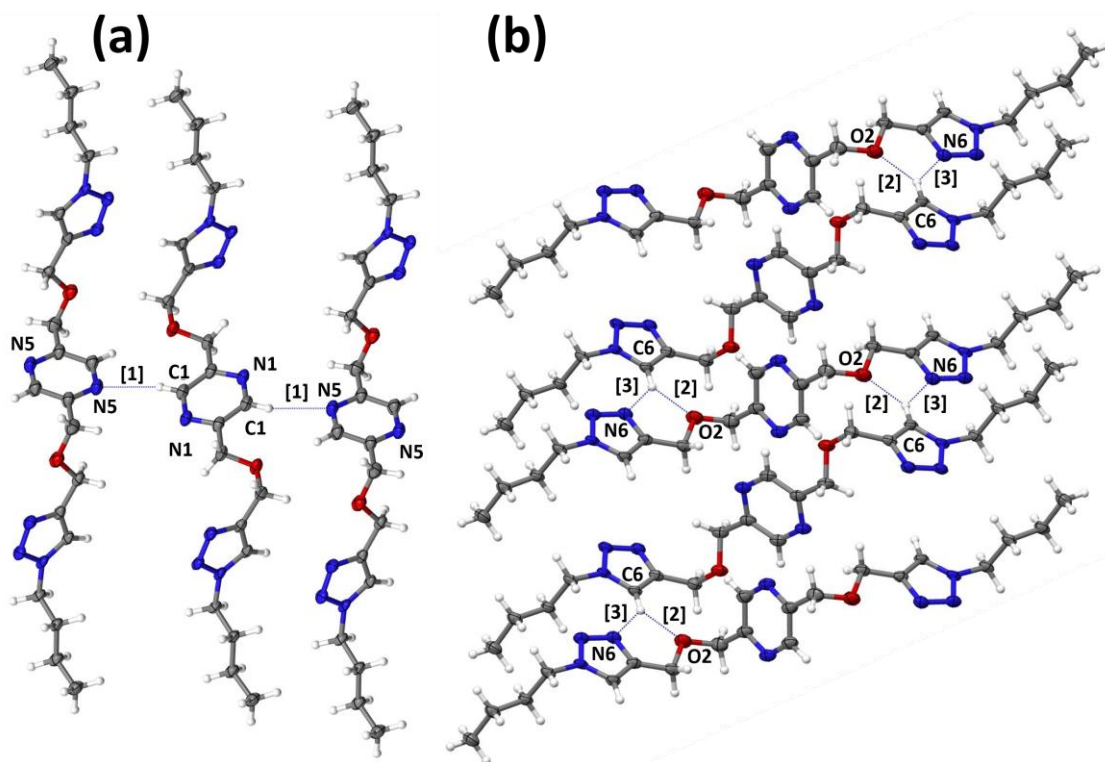
X-ray crystal structure of L2: 2,5-bis(((1-butyl-1H-1,2,3-triazol-4-yl)methoxy)methyl)pyrazine

White needle-like crystals suitable for single-crystal X-ray diffraction analysis were obtained from the addition of water into a methanolic solution of **L2**. The data was solved and refined in the triclinic space group $P\bar{1}$ with the asymmetric unit containing two separate **L2** fragments. Crystallographic symmetry generates rows of ligands of alternating orientations about the central pyrazine (Fig. S5). The two fragments in the asymmetric unit adopt different Z-shaped conformations, with the ‘bend’ of the ligand occurring in different sides of the ether oxygen atom. The O1 oxygen lies relatively planar to the N1 pyrazine with a C1-C2-C3-O1 dihedral of 27.5(3)°, and relatively perpendicular to the N2 triazole with an O1-C4-C5-C6 dihedral of 76.2(3)°, compared to the second ligand orientation where the O2 ether oxygen lies more perpendicular to its N5 pyrazine with a C11-C12-C13-O2 dihedral of 61.7(3)° and more planar to the N6 triazole, with an O2-C14-C15-N6 dihedral of 8.4(2)°.

Crystal Data for $\text{C}_{20}\text{H}_{30}\text{N}_8\text{O}_2$ ($M = 414.52$ g/mol): triclinic, space group $P\bar{1}$ (no. 2), $a = 4.5792(4)$ Å, $b = 9.5207(8)$ Å, $c = 24.601(2)$ Å, $\alpha = 86.182(4)^\circ$, $\beta = 86.199(4)^\circ$, $\gamma = 81.258(4)^\circ$, $V = 1056.02(16)$ Å 3 , $Z = 2$, $T = 100$ K, $\mu(\text{CuK}\alpha) = 0.722$ mm $^{-1}$, $\rho_{\text{calc}} = 1.304$ g/cm 3 , 15004 reflections measured ($7.214^\circ \leq 2\theta \leq 130.154^\circ$), 3565 unique ($R_{\text{int}} = 0.0559$,

$R_{\text{sigma}} = 0.0481$) which were used in all calculations. The final R_1 was 0.0961 ($I \geq 2\sigma(I)$) and wR_2 was 0.2957 (all data).

Figure S5 The (a) intermolecular pyrazine...pyrazine hydrogen bonding interactions [1] (shown using



a blue line) of parallel molecules, between alternating orientations of adjacent pyrazine and (b) the triazole...triazole hydrogen bonding interactions between layers of molecules [2] and [3] (shown using blue lines). Ellipsoids are drawn at the 50% probability level.

The ligands are held together by intermolecular hydrogen bonding interactions between the two pyrazine centres of the alternate ligand arrangements, with the C1 pyrazine carbon of one ligand donating a hydrogen bond to the N5 pyrazine nitrogen of the other ligand, with an C...N of 3.391(4) Å and a C-H...N angle of 163.01(16)°, (Fig. S5). Additional intermolecular hydrogen bonding interactions exist between the C6 triazole carbon donating to the O2 ether oxygen and N6 triazole nitrogen of the alternately bent arms of the neighbouring ligands, which generate a three-dimensional intermolecular network, (Table 2).

Table: The bond lengths (Å) and angles (°) of the intermolecular forces between **L2** ligands in Figure S5

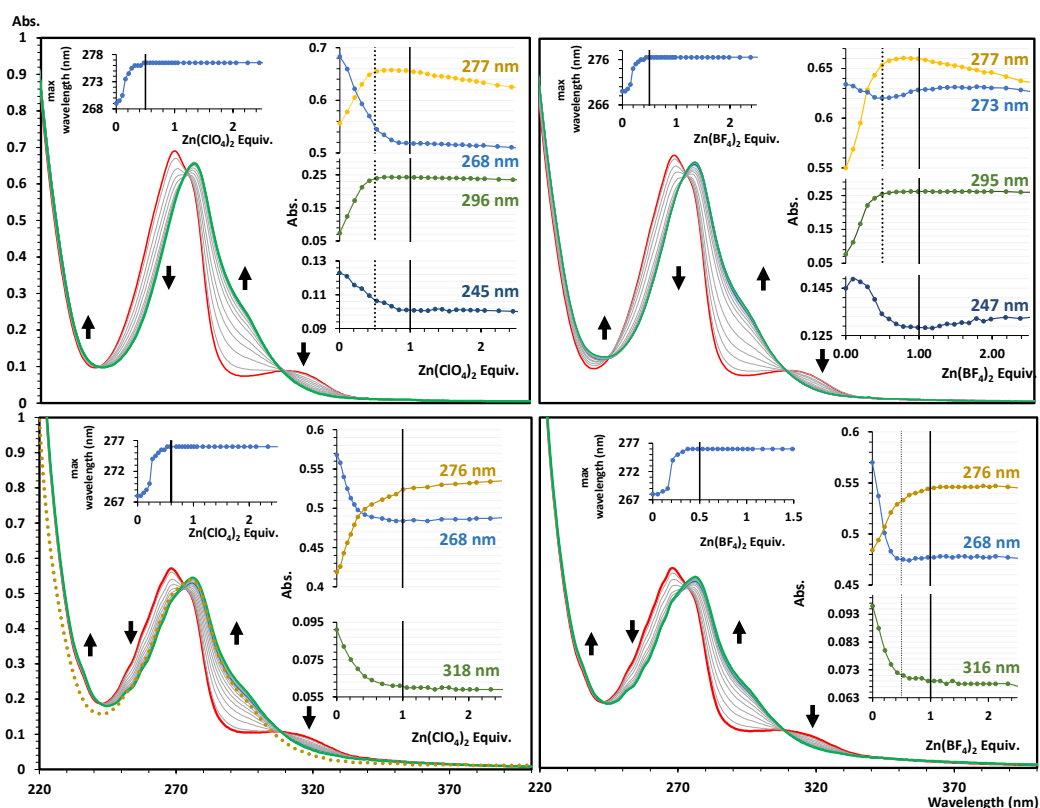
	D-H...A	D-H/Å	H...A/Å	D...A/Å	D-H...A/°
[1]	C1-H1...N5	0.950 (3)	2.471 (2)	3.391 (4)	163.01 (16)
[2]	C6-H6...O2	0.950 (3)	2.4922 (19)	3.351 (3)	150.43 (15)
[3]	C6-H6...N6	0.950 (3)	2.619 (2)	3.369 (4)	136.10 (17)

S1.4 SCXRD of organic compounds

Identification code	2	L2
Empirical formula	C ₁₀ H ₁₂ N ₂ O ₄	C ₂₀ H ₃₀ N ₈ O ₂
Deposition No.	2301236	2301237
Formula weight	224.22	414.52
Temperature / K	100.00	100.00
Crystal system	monoclinic	triclinic
Space group	<i>P</i> 2 ₁ / <i>c</i>	<i>P</i> $\bar{1}$
<i>a</i> / Å	11.3960(17)	4.5792(4)
<i>b</i> / Å	5.4689(8)	9.5207(8)
<i>c</i> / Å	8.3487(13)	24.601(2)
<i>α</i> / °	90	86.182(4)
<i>β</i> / °	90.197(9)	86.199(4)
<i>γ</i> / °	90	81.258(4)
Volume / Å³	520.32(14)	1056.02(16)
<i>Z</i>	2	2
ρ_{calc} / g cm⁻³	1.431	1.304
μ / mm⁻¹	0.949	0.722
F(000)	236.0	444.0
Crystal size / mm	0.1 × 0.04 × 0.02	0.27 × 0.07 × 0.02
Radiation	CuK α (λ = 1.54178)	CuK α (λ = 1.54178)
2θ range for data collection / °	7.758 to 136.37	7.214 to 130.154
Index ranges	-13 ≤ <i>h</i> ≤ 13, -6 ≤ <i>k</i> ≤ 6, -10 ≤ <i>l</i> ≤ 10	-5 ≤ <i>h</i> ≤ 5, -10 ≤ <i>k</i> ≤ 11, -28 ≤ <i>l</i> ≤ 28
Reflections collected	5326	15004
Independent reflections	927 [R _{int} = 0.0966, R _{sigma} = 0.0662]	3565 [R _{int} = 0.0559, R _{sigma} = 0.0481]
Data/restraints/parameters	927/0/76	3565/0/273
Goodness-of-fit on F²	1.166	1.250
Final R indexes [<i>I</i> ≥ 2σ(<i>I</i>)]	R ₁ = 0.0780, wR ₂ = 0.2125	R ₁ = 0.0961, wR ₂ = 0.2734
Final R indexes [all data]	R ₁ = 0.0807, wR ₂ = 0.2152	R ₁ = 0.1093, wR ₂ = 0.2957
Largest diff. peak/hole / e Å⁻³	0.80/-0.42	1.24/-0.39

S2 Characterization of Products

S2.1 UV-Vis Spectroscopy



UV-vis spectroscopy titration experiments: (Top Left) stepwise addition of 6.1 μL of $5 \times 10^{-3} \text{ mol L}^{-1}$ of solution of $\text{Zn}(\text{BF}_4)_2$ to a $9.5 \times 10^{-5} \text{ mol L}^{-1}$ of **L2** in CH_3CN . (Top Right) stepwise addition of 6.1 μL of $5 \times 10^{-3} \text{ mol L}^{-1}$ of solution of $\text{Zn}(\text{ClO}_4)_2$ to a $9.5 \times 10^{-5} \text{ mol L}^{-1}$ of **L2** in CH_3CN . (Bottom Left) stepwise addition of 3.2 μL of $5 \times 10^{-3} \text{ mol L}^{-1}$ of solution of $\text{Zn}(\text{ClO}_4)_2$ to a $9.42 \times 10^{-5} \text{ mol L}^{-1}$ of **L4** in CH_3CN . (Bottom Right) stepwise addition of 3.2 μL of $5 \times 10^{-3} \text{ mol L}^{-1}$ of solution of $\text{Zn}(\text{BF}_4)_2$ to a $9.42 \times 10^{-5} \text{ mol L}^{-1}$ of **L4** in CH_3CN .

Where the red represents 0 equiv. Zn^{2+} blue is 0.5 Zn^{2+} equiv. and green 1 Zn^{2+} equiv. added. The inset graphs show the changes in the absorption with the increase of the amount of transition metal ions. The dashed yellow data in graph c represents $1.12 \times 10^{-7} \text{ mol L}^{-1}$ of complex **4a** in MeCN, scaled to the peak of the one Zn^{2+} equiv. indicating the formation of the polymer.

S2.2 L1 and L2 complexes

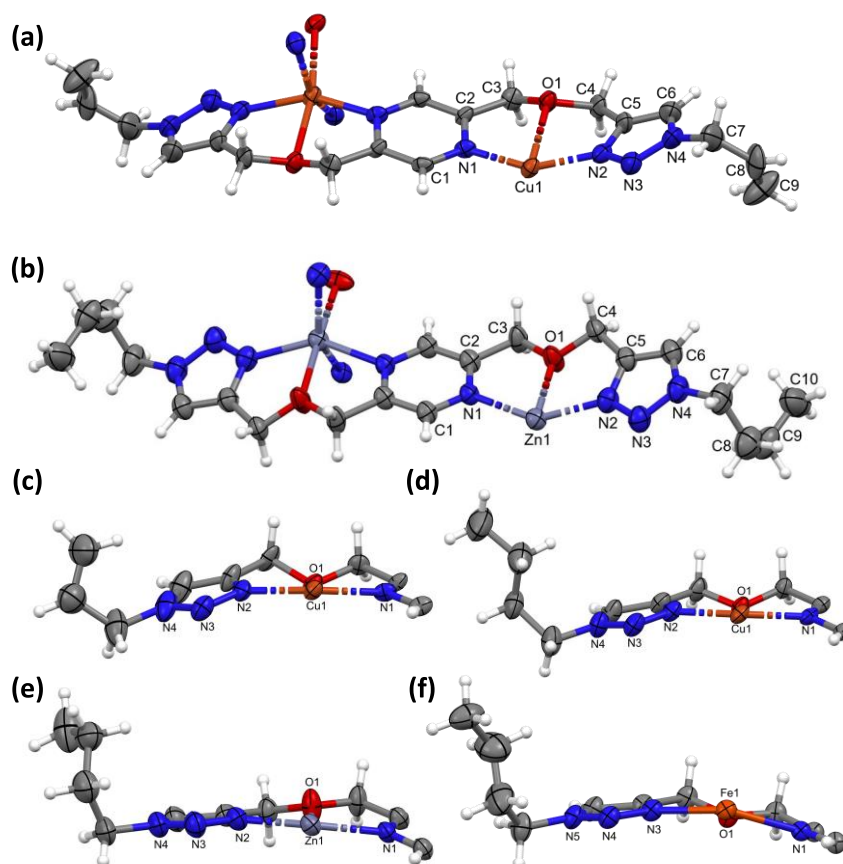


Figure S 6 A perspective view of a section of the x-ray structures of (a) the **L1** complex **1A** and (b) the **L2** complex **2A** (which is isostructural with **2B** and **2C**) with the asymmetric unit labelled. Counterions have been removed for clarity. A summary view of the CP complexes illustrating the variation in the alkyl end-group arrangement, and the N1-M-N2-O1 torsion in (c) **1A**; (d) **2C**; (e) **2A**; and (f) **2B**. Ellipsoids are drawn at the 50% probability level.

With regards to the complexes assembled from the alkyl-end-group ligands **L1** and **L2**, all four complexes were solved and refined in centrosymmetric monoclinic space groups: $C2/c$ (for **1A**, **2A** and **2C**) and $P2_1/n$ (for **2B**), where **1A**, **2A** and **2C** had an asymmetric unit of one half of an **L2** ligand coordinated to a half-occupancy of an M^{2+} ion, with an associated counterion, while **2B** had an asymmetric unit of one **L2** ligand coordinated to a single Fe^{2+} centre, with two associated perchlorate ions. Additionally, in complex **1A** the end two carbon atoms of the propene end group of the **L1** ligand are spatially disordered in a 1:1 ratio, and in complex **2c** the middle two carbon atoms of the **L2** butyl end group are disordered in a 1:3 ratio.

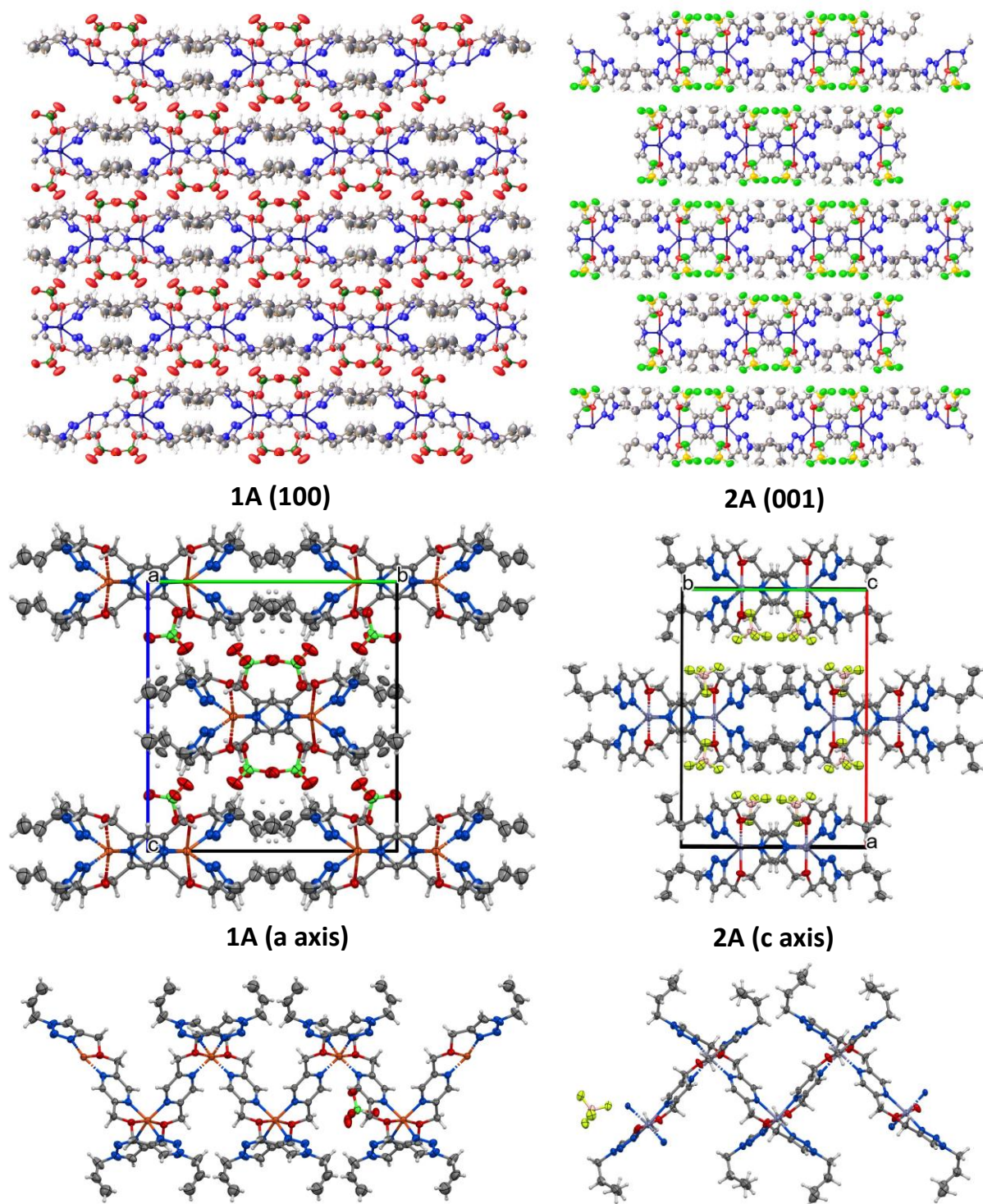
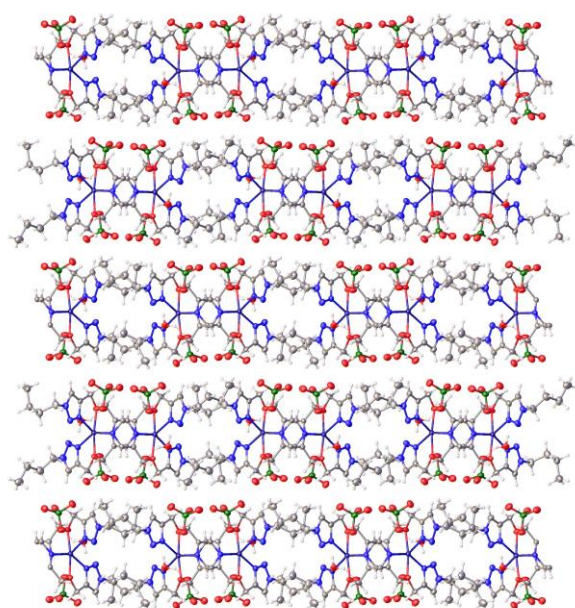
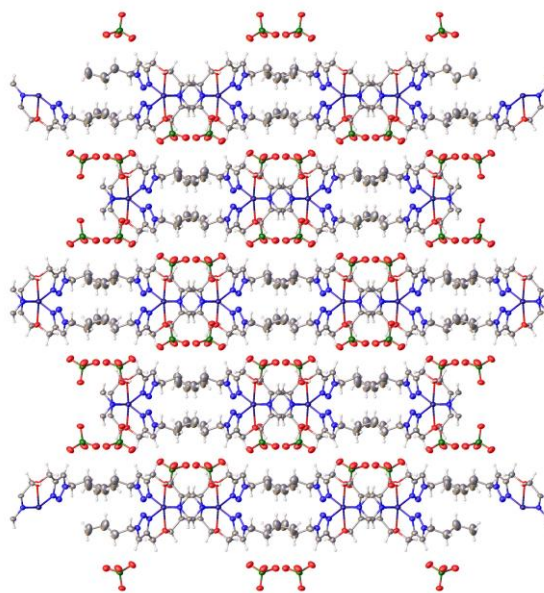


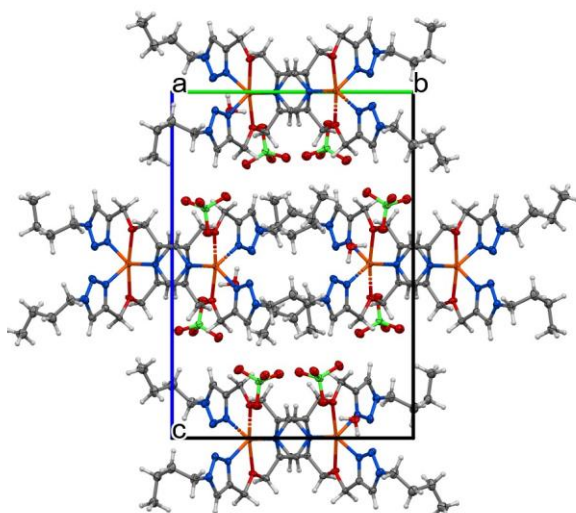
Figure S 7 Left hand side: the (100) view; a view down the a-axis; and a view of the **1A** complex polymer. Right hand side: the (001) view; a view down the c-axis; and a view of the **2A** complex polymer



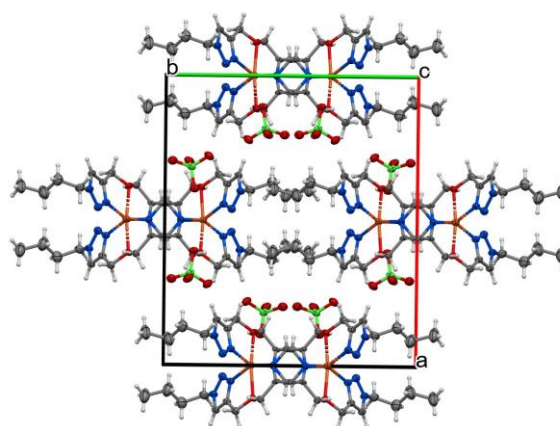
2B (100)



2C (001)



2B (a axis)



2C (c axis)

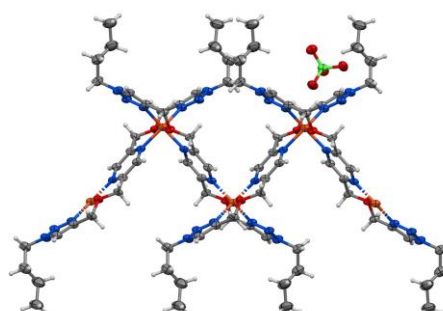
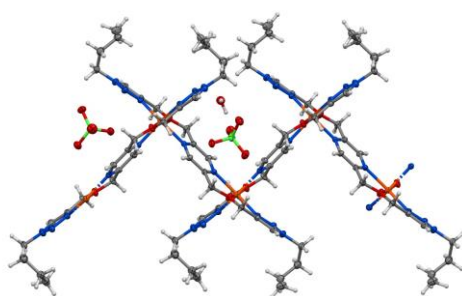
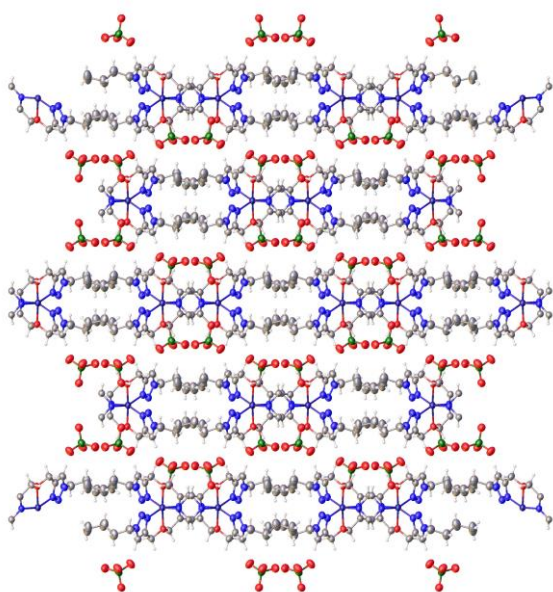
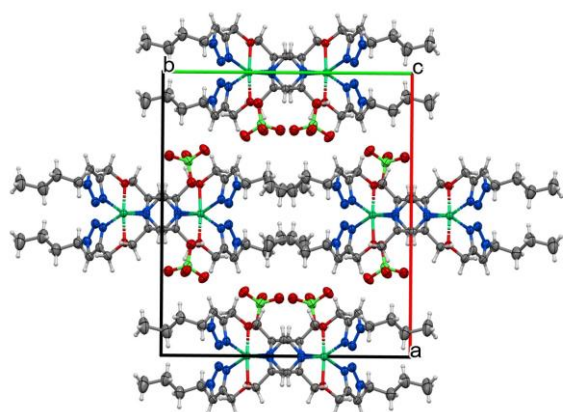


Figure S 8 Left hand side: the (100) view; a view down the a-axis; and a view of the **2B** complex polymer. Right hand side: the (001) view; a view down the c-axis; and a view of the **2C** complex polymer



2D (001)



2D (c axis)

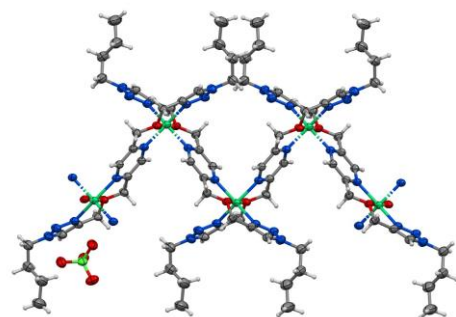


Figure S 9 The (001) view; a view down the c-axis; and a view of the **2D** complex polymer

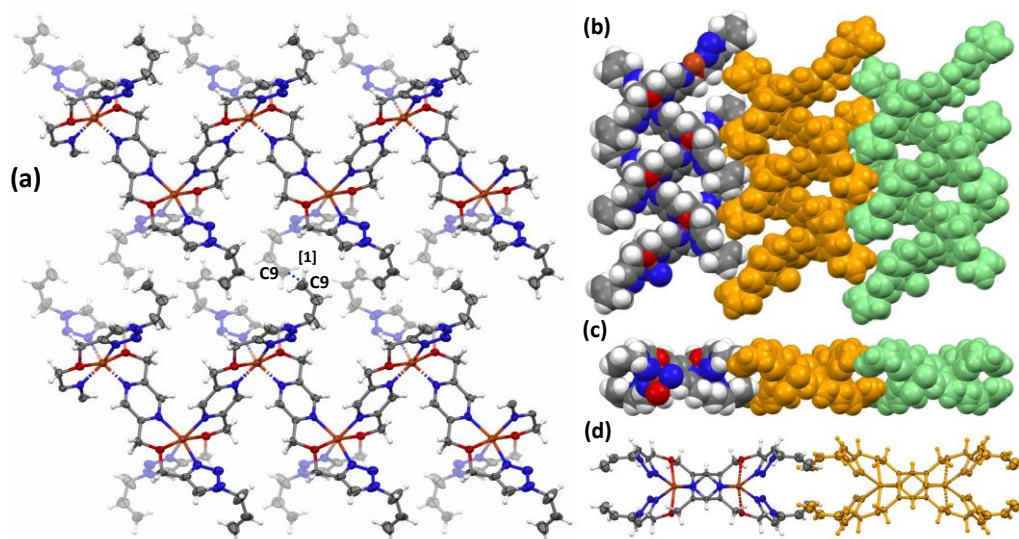


Figure S 10 A perspective view of a section of the zig-zag polymer strands of complex **1A**, analogous to the other ligand **L1** complexes. The perchlorate anions have been removed for clarity. (a) With the distance of 3.66(7) Å between neighbouring C9 alkene carbons of adjacent CPs [1]. A perspective view of the sphere packing of a 2D sheets formed by the overlapping of alkyl tails of adjacent coordination polymer chains, as seen down (b) the a-axis and (c and d) the c-axis. The left-most CP is coloured by element, while the middle chain (orange) and right-most chain (green) are coloured to more easily see the overlapping alkyl groups. Ellipsoids are drawn at the 50% probability level.

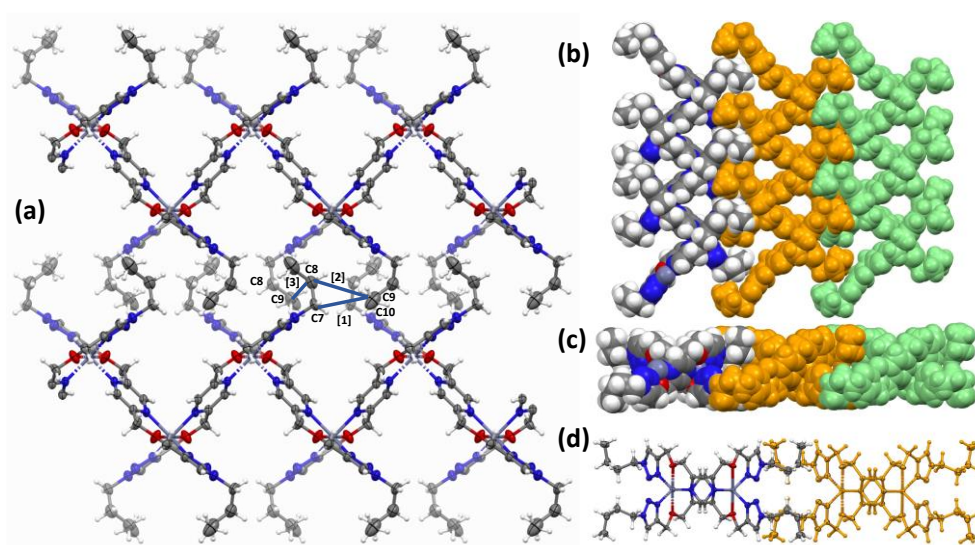


Figure S11 A perspective view of a section of the zig-zag polymer strands of complex **2A**, analogous to the other ligand **L2** complexes. The perchlorate anions have been removed for clarity. A perspective view down the a-axis (a) in an ellipsoidal view, and (b) a sphere packing view, of a section of the zig-zag polymer strands of complex, where the butyl end groups are held closely together with distances of [1] C7-C9¹ 3.735 (7); [2] C8-C9¹ 4.037 (8); and C8-C9² 4.171 (10) Å. A view down the c-axis (c) in an ellipsoidal view, and (d) a sphere packing view, of a 2D sheets formed by the overlapping of alkyl tails of adjacent coordination polymer chains.

S2.3 L3 Complexes

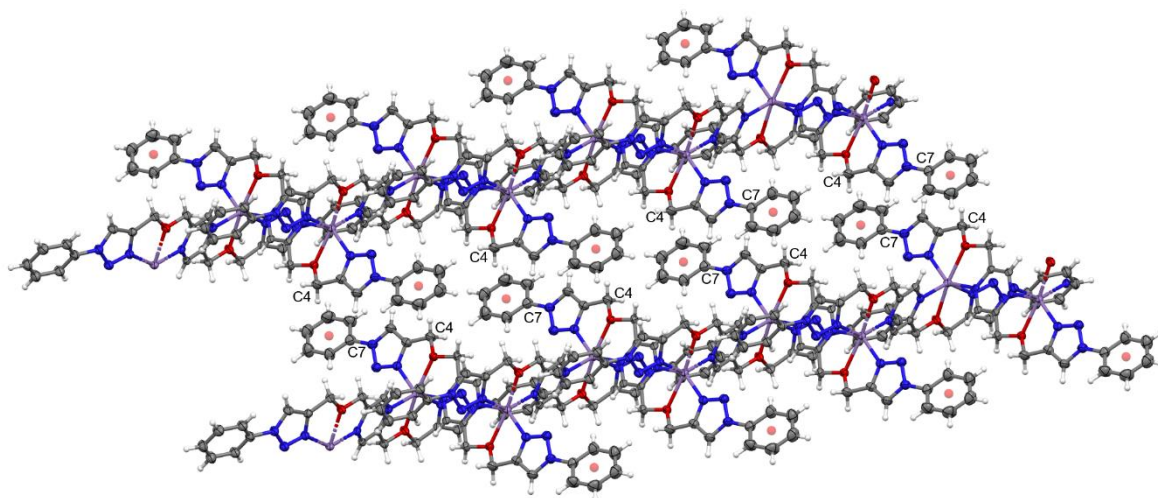


Figure S 12 An ellipsoidal view of the length of a 1D polymer chain. The intermolecular CH- π interactions between the calculated C7-C13 phenyl centroid (shown as a red sphere) and the C4 carbon of an adjacent chain, resulting in the overlap of planar ligands of adjacent polymer chains of the **3A** complex.

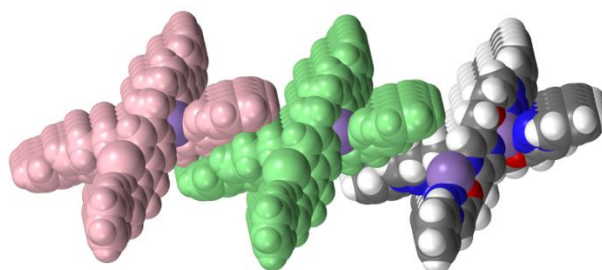


Figure S 13 A perspective view down the a-axis of polymer strands of the **3A** complex in a sphere packing view. Perchlorate anions have been removed for clarity.

S2.4 L4 Complexes

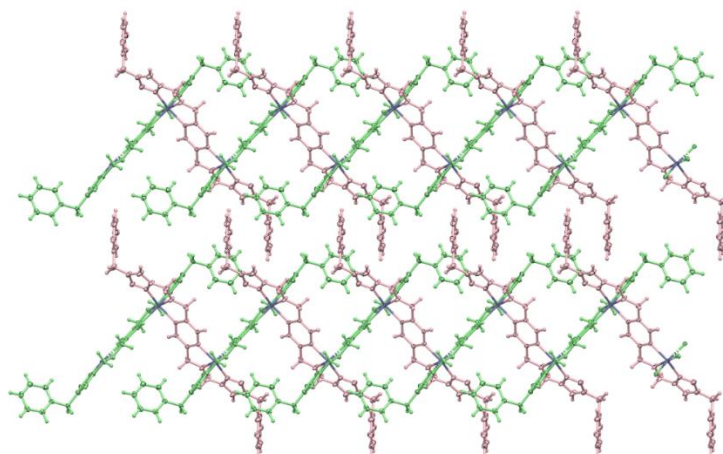


Figure S 14 A perspective view of two polymer chains of **4A** 'zipped' together by the π - π interactions of the C21-C26 centroid of the perpendicular ligands (coloured pink) with the off-set ligands (coloured green) (b) shown in 50% probability level ellipsoids

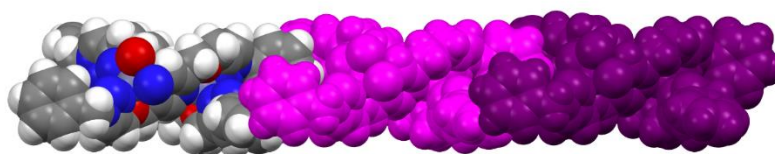


Figure S 15 A sphere packing view of the interlocked polymer chains of **4A** in a 2D sheet – separate polymer chains are coloured for clarity.

S2.5 Powder XRD spectra

Powder XRD was investigated as a technique for determining sample purity for bulk quantities. Samples tested; **1A**, **2A** and **4B**, resulted in patterns that indicate structures corresponding to the crystalline polymer materials exhibited by the SCXRD data.

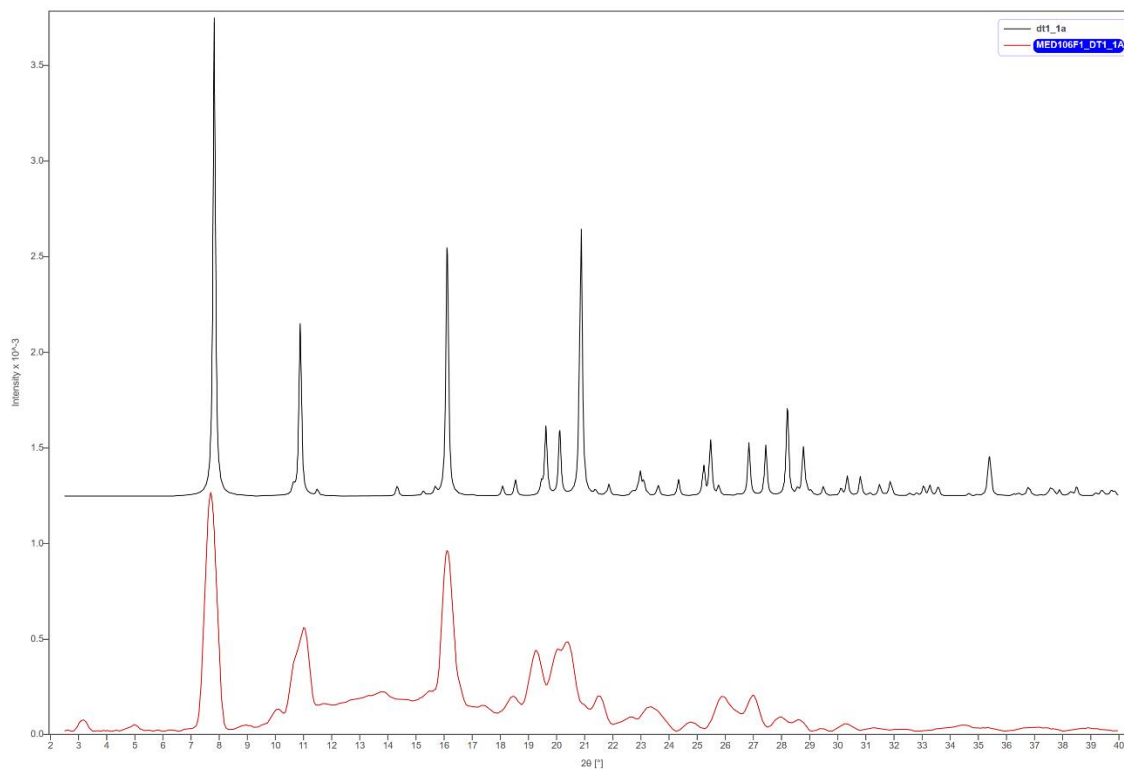


Figure S 16 The comparison between the calculated and experimental PXR spectra for **1A**.

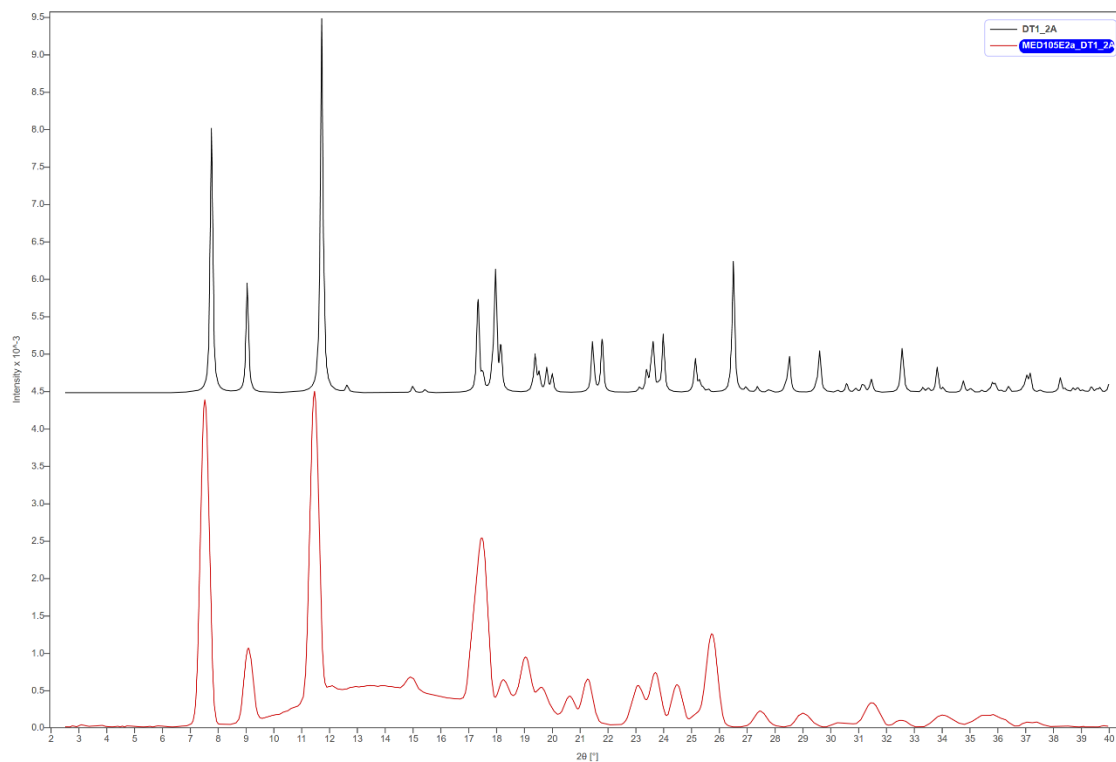


Figure S 17 The comparison between the calculated and experimental PXRD spectra for **2A**.

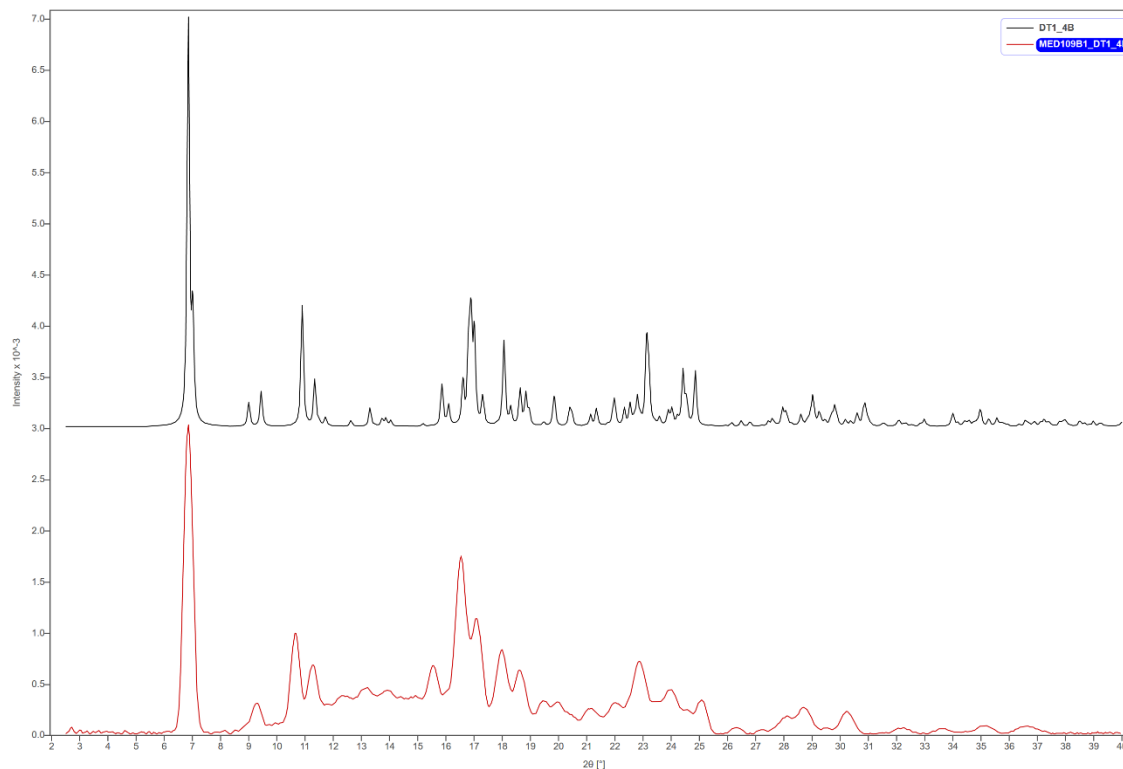


Figure S 18 The comparison between the calculated and experimental PXRD spectra for **4B**.

S3 NMR Spectra

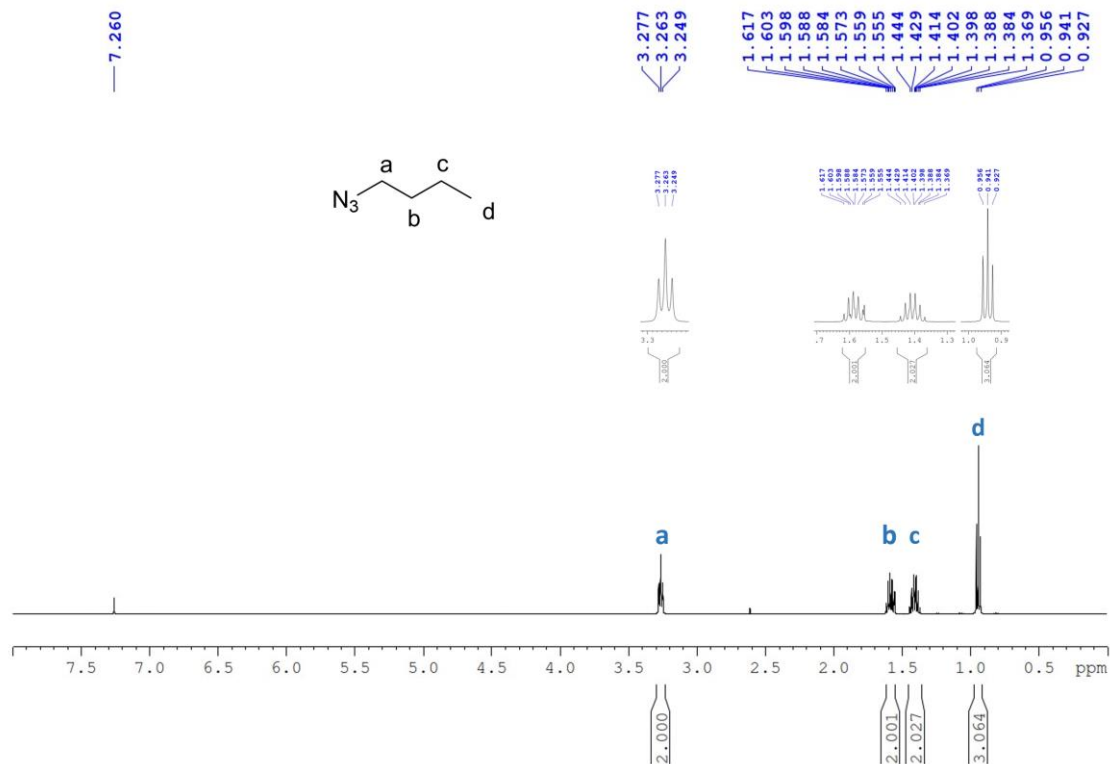


Figure S19. ^1H NMR spectrum of azido butane in CDCl_3 .

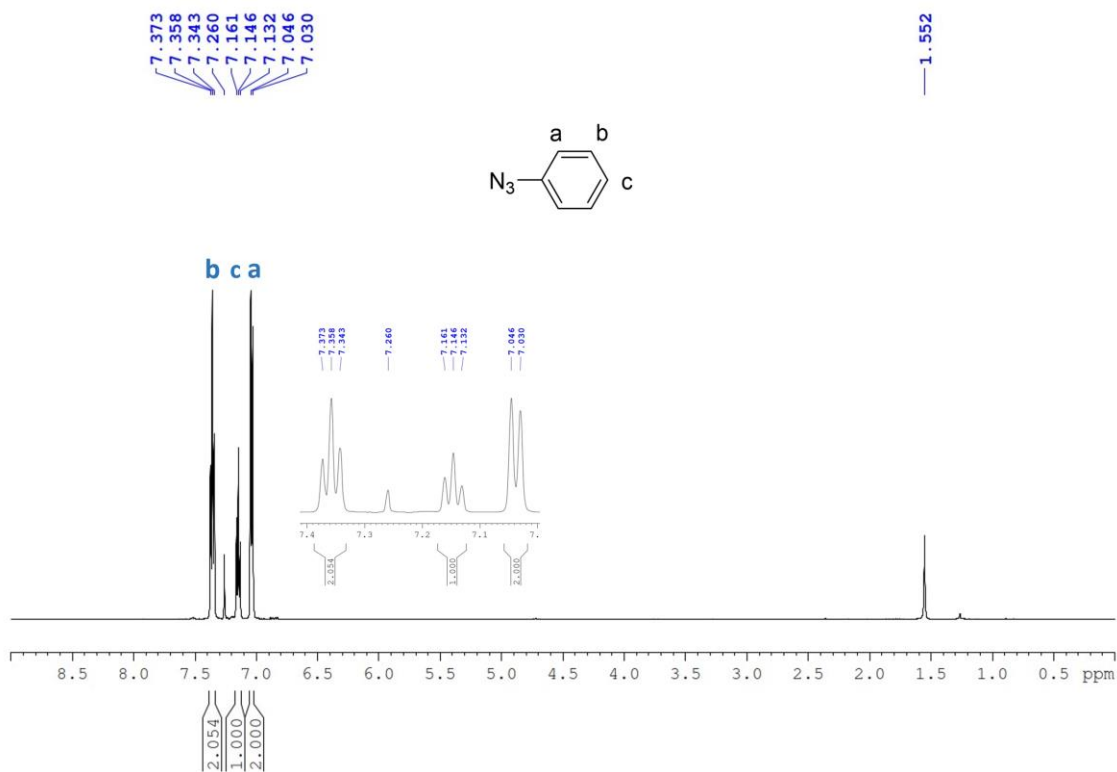


Figure S20 ^1H NMR spectrum of phenyl azide in CDCl_3 .

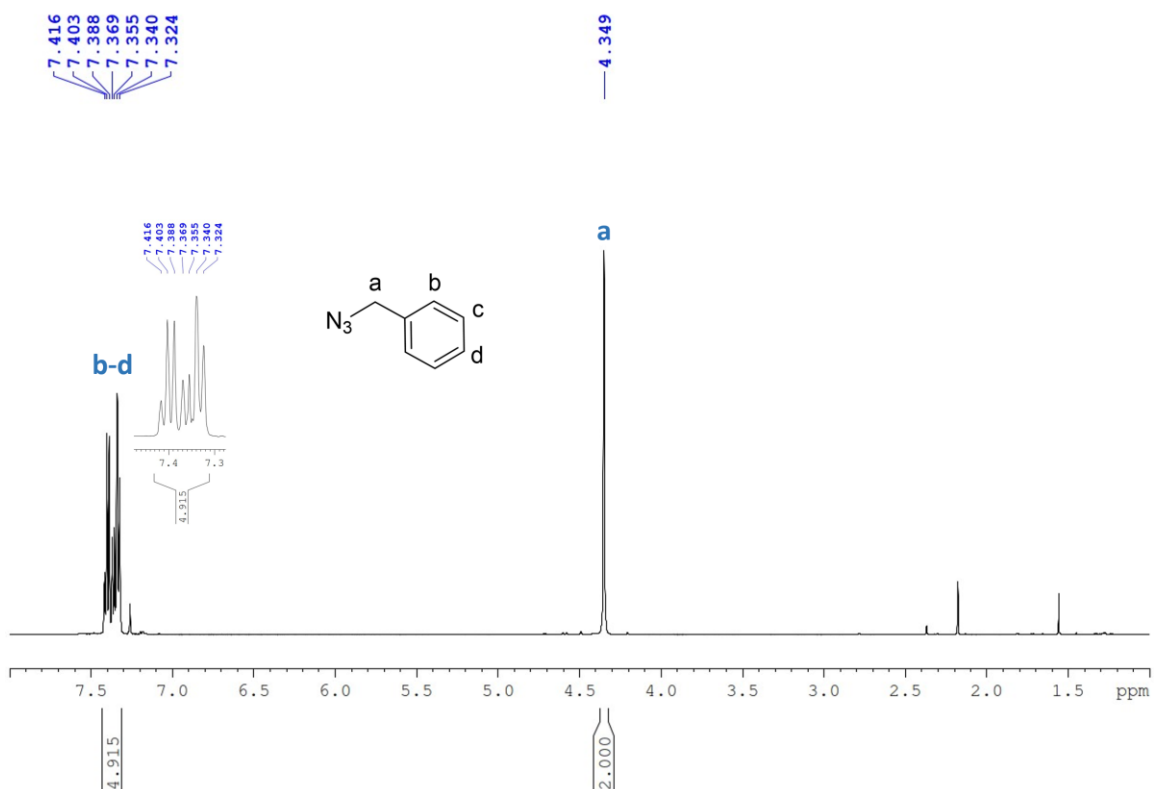


Figure S21 ^1H NMR spectrum of benzyl azide in CDCl_3 .

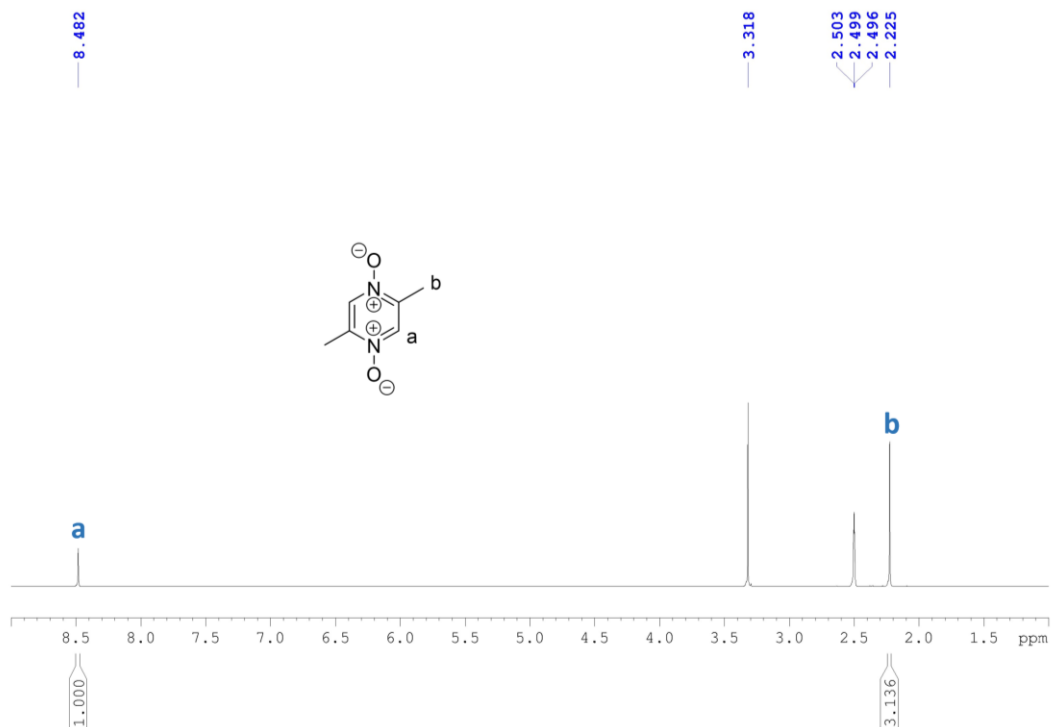


Figure S22 ^1H NMR spectrum of 2,5-dimethylpyrazine-1,4-N-oxide (**1**) in DMSO-d_6 .

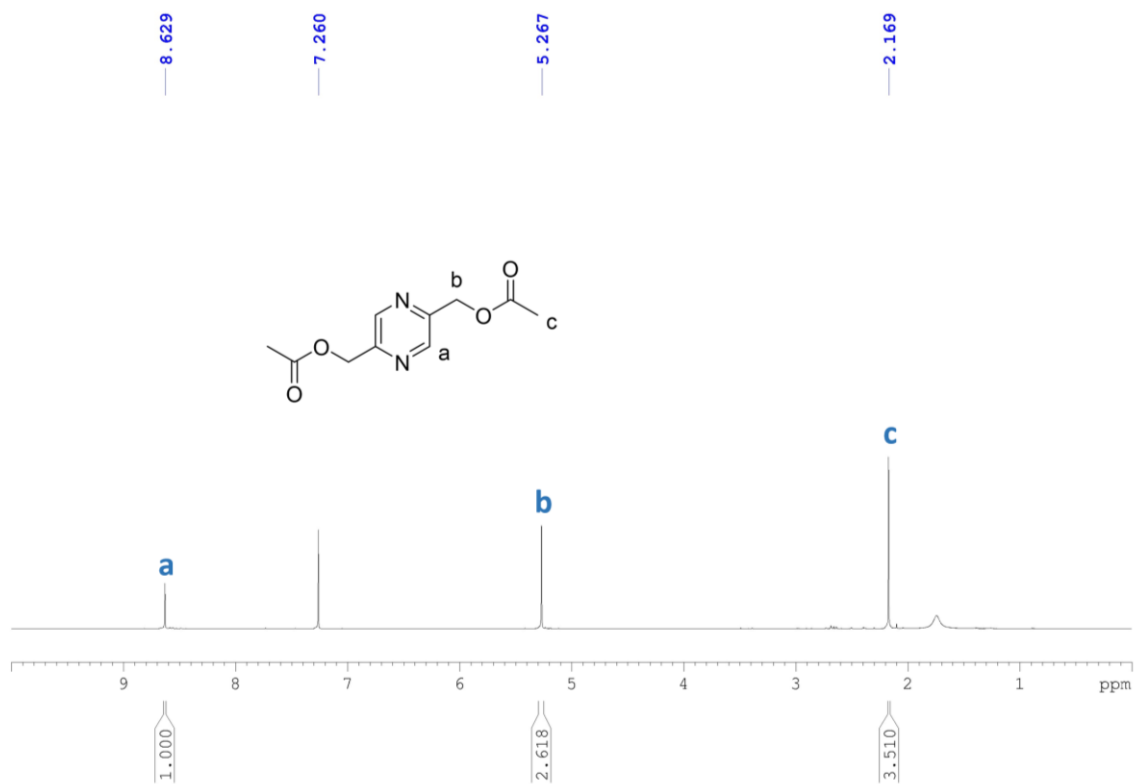


Figure S23 ¹H NMR spectrum of 2,5-bis(acetoxymethyl)pyrazine (**2**) in CDCl₃.

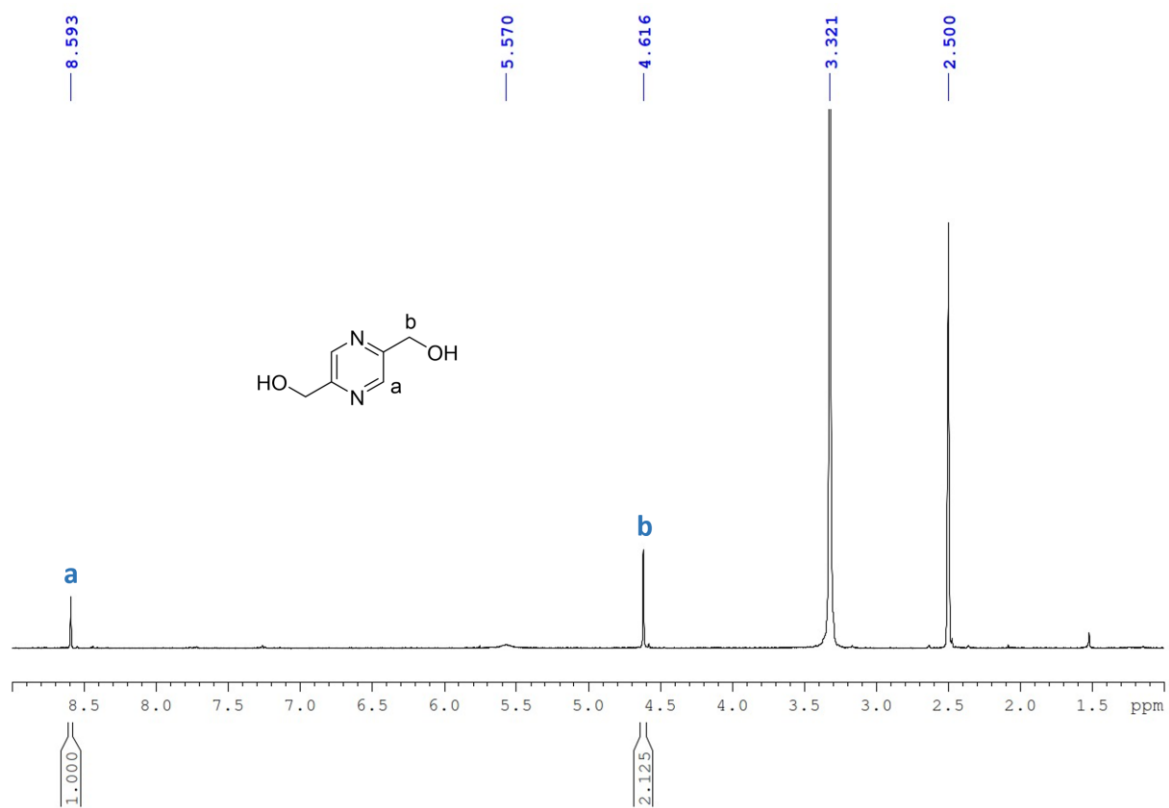


Figure S24 ¹H NMR spectrum of 2,5-bis(hydroxymethyl)pyrazine (**3**) in DMSO-d₆.

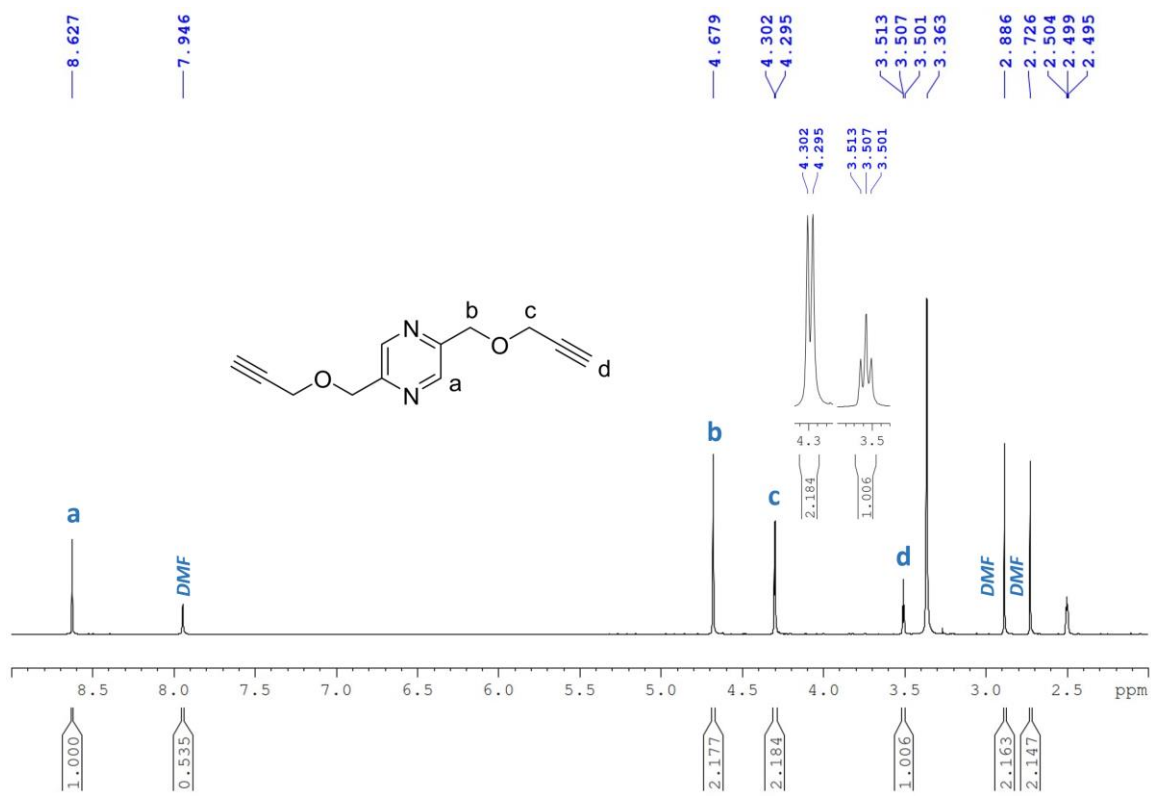


Figure S25 ¹H NMR spectrum of 2,5-bis((prop-2-yn-1-yloxy)methyl)pyrazine (**4**) in DMSO-d₆.

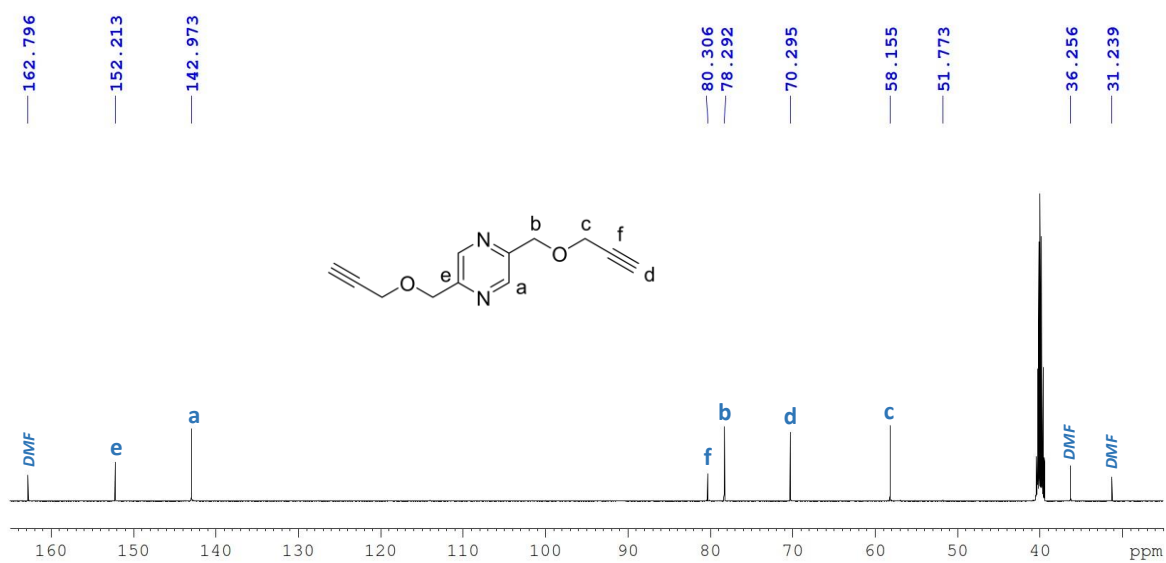


Figure S26 ¹³C NMR spectrum of 2,5-bis((prop-2-yn-1-yloxy)methyl)pyrazine (**4**) in DMSO-d₆.

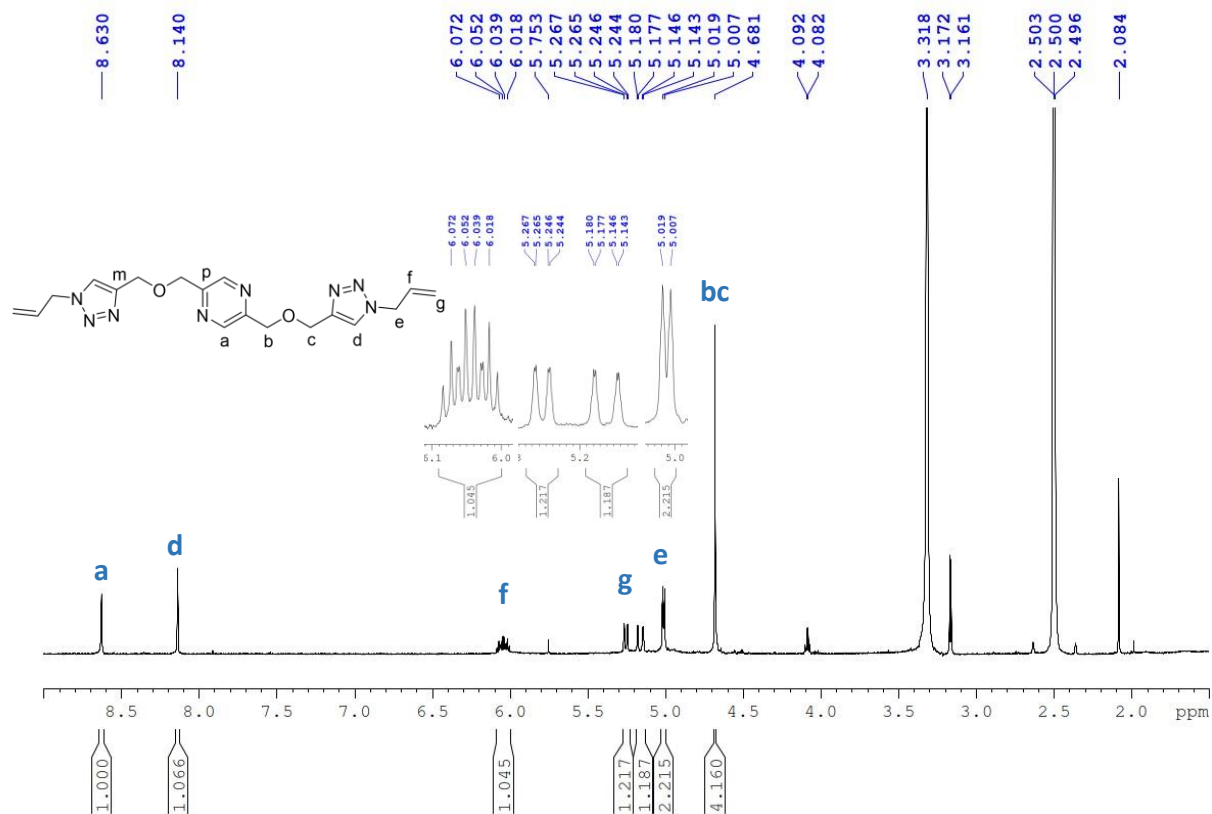


Figure S27 ^1H NMR spectrum of **L1** in DMSO-d_6 .

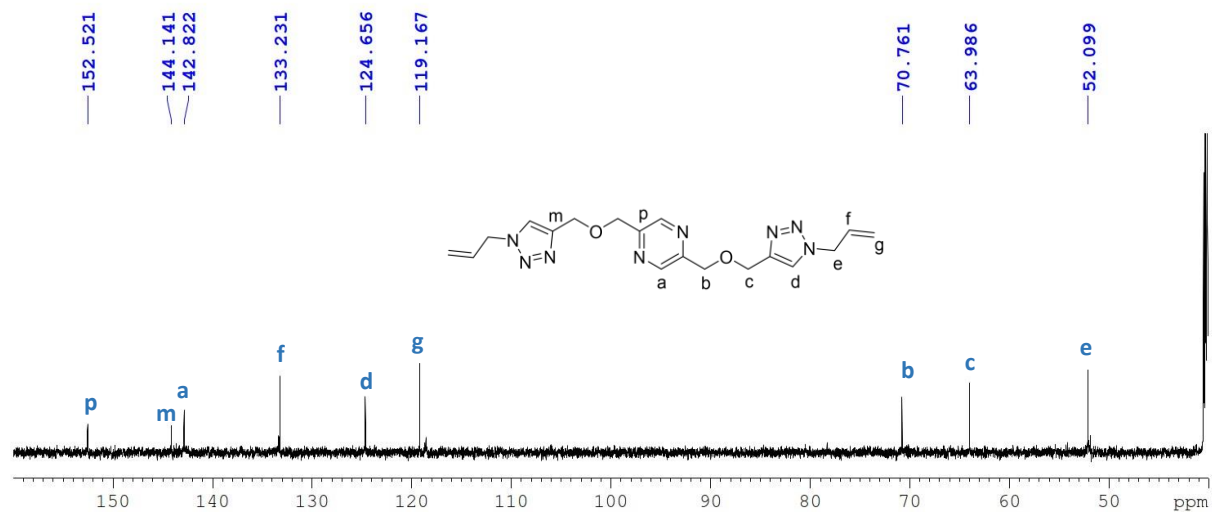


Figure S28 ^{13}C NMR spectrum of **L1** in DMSO-d_6 .

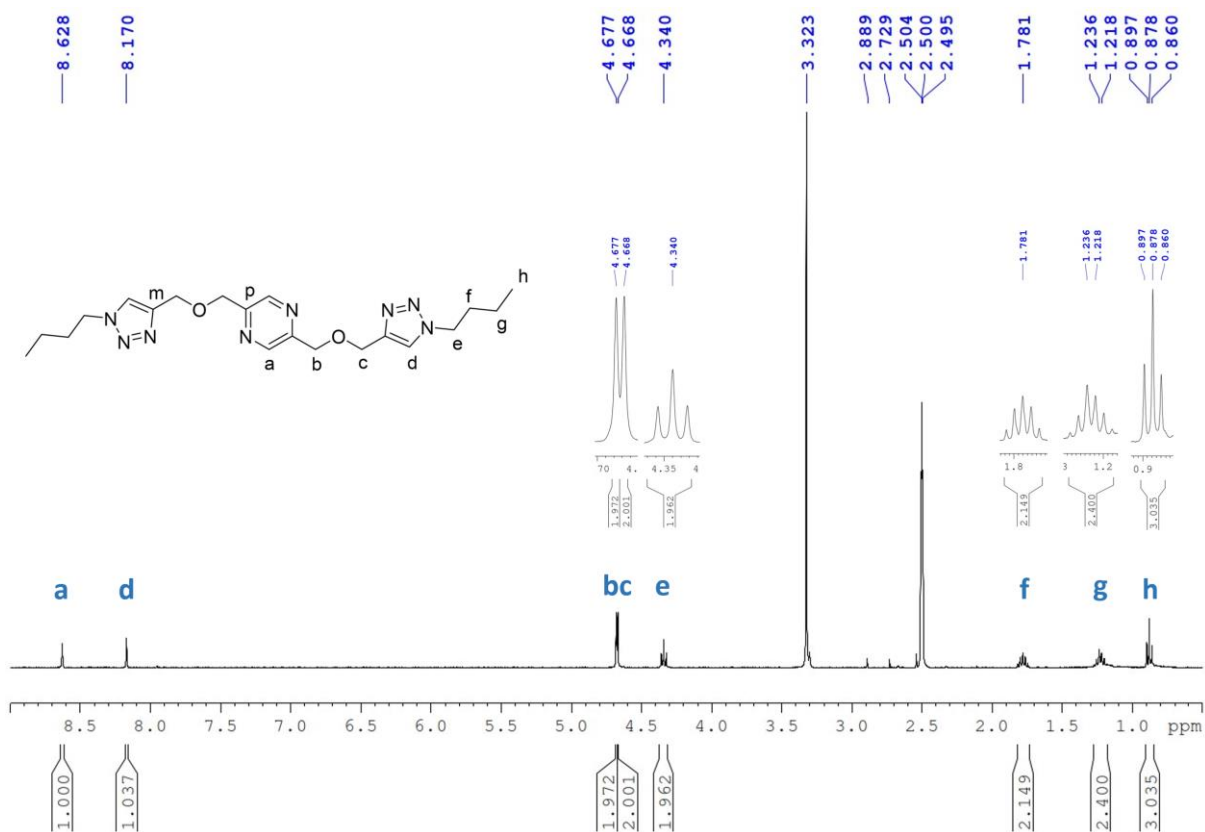


Figure S29 ^1H NMR spectrum of **L2** in DMSO-d_6 .

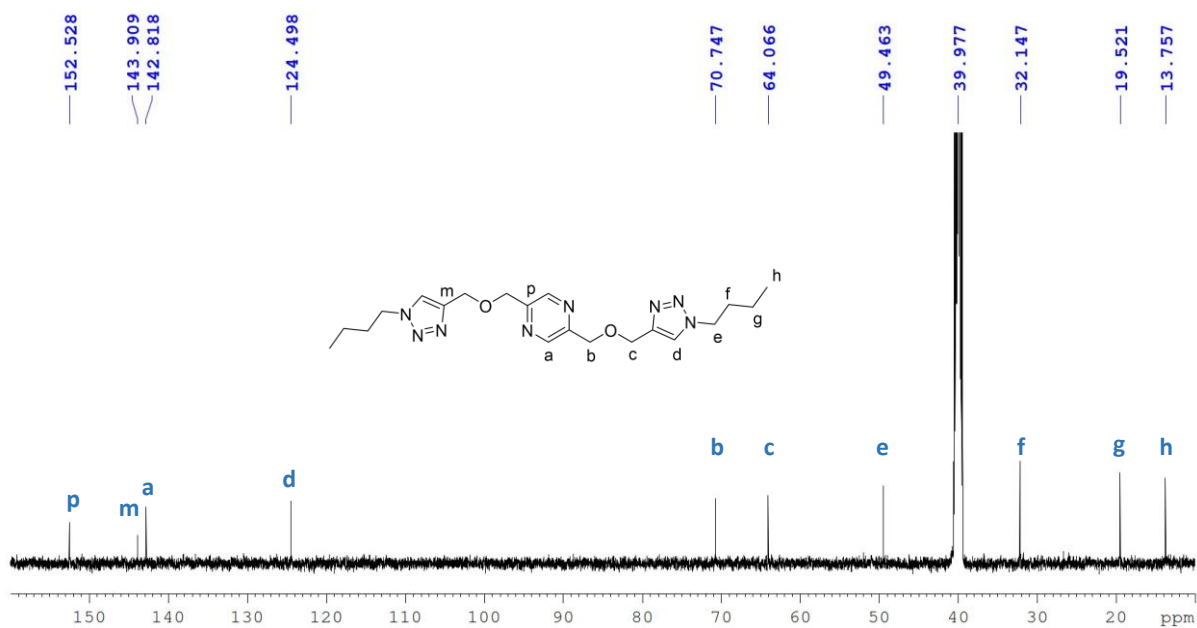


Figure S30 ^{13}C NMR spectrum of **L2** in DMSO-d_6 .

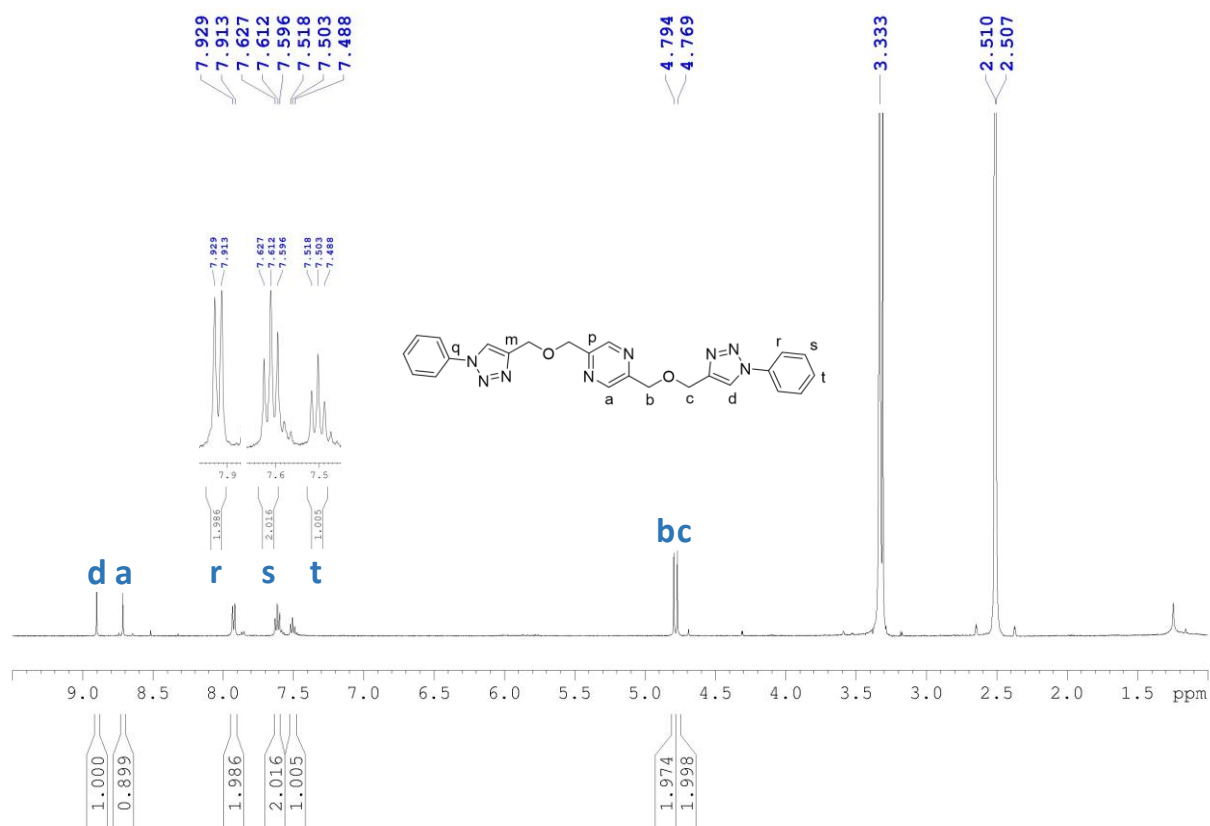


Figure S31 ¹H NMR spectrum of **L3** in DMSO-d₆.

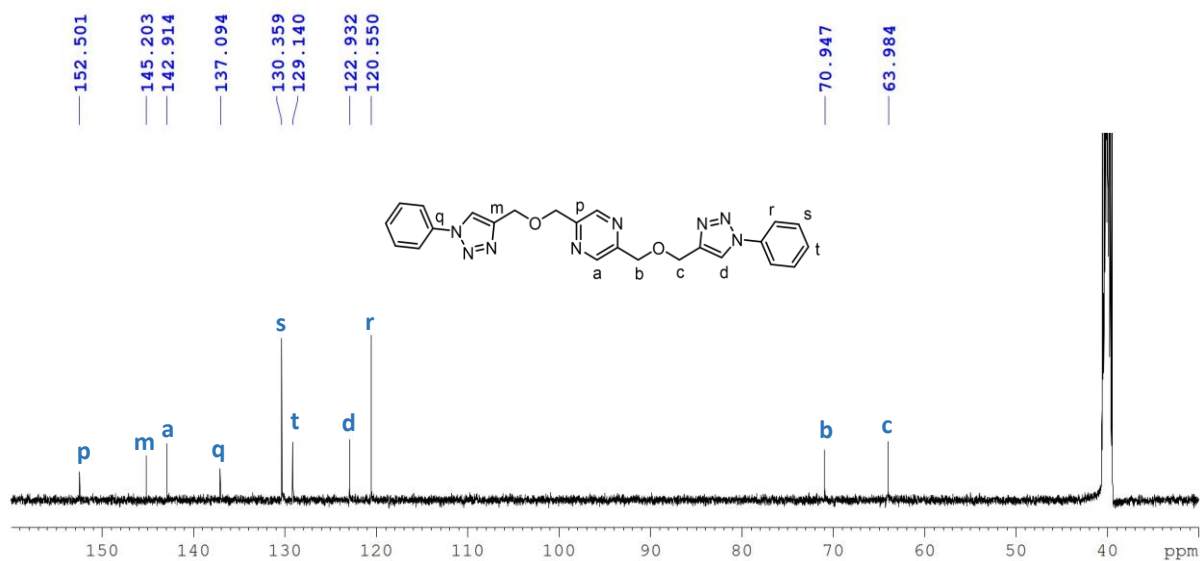


Figure S32 ¹³C NMR spectrum of **L3** in DMSO-d₆.

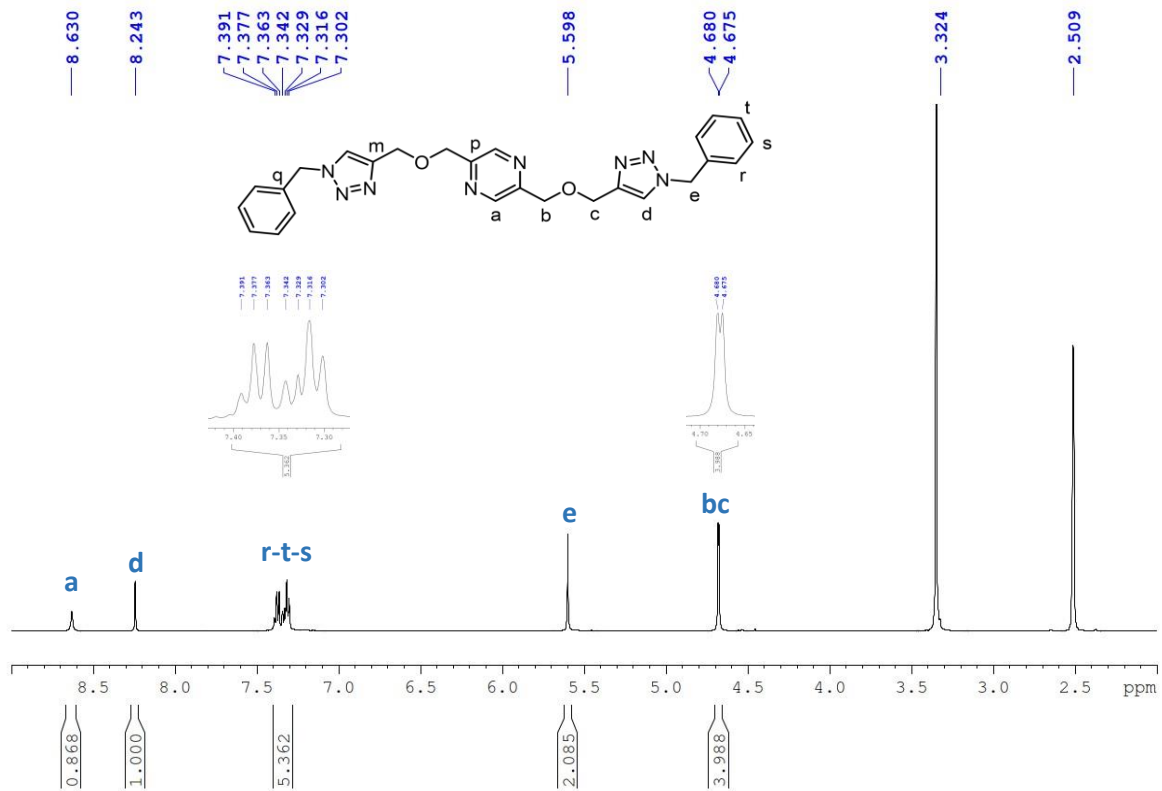


Figure S 33 ^1H NMR spectrum of L4 in DMSO.

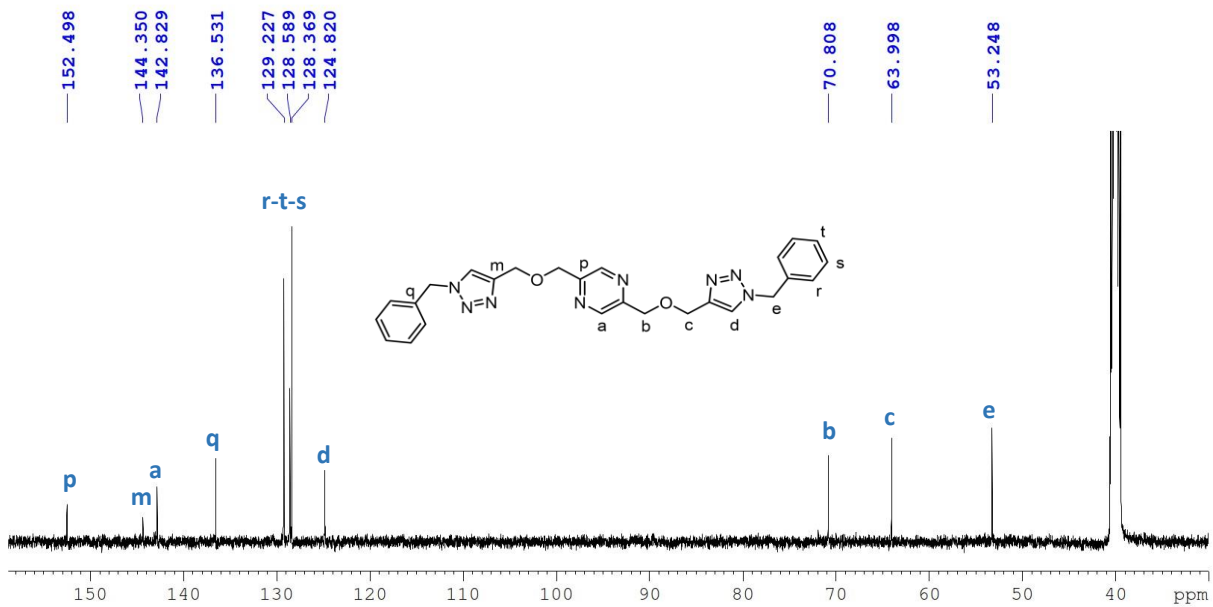


Figure S 34 ^{13}C NMR spectrum of L4 in DMSO.

S4 Infrared Spectra

S4.1 ATR-IR : organic precursors and ligands

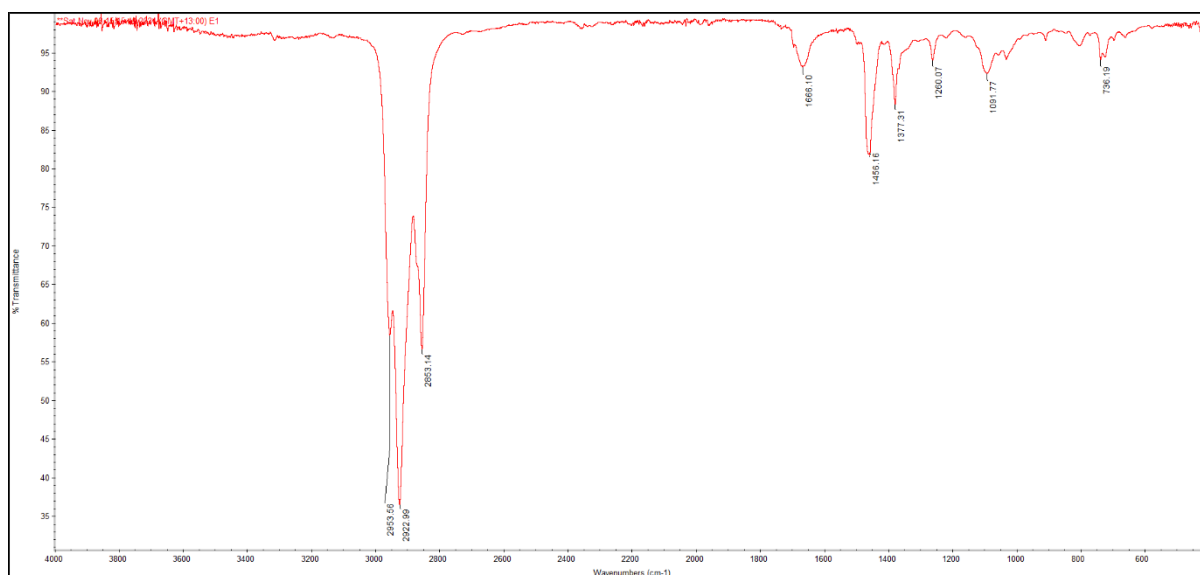


Figure S 35 ATR-IR of alkyne compound 4

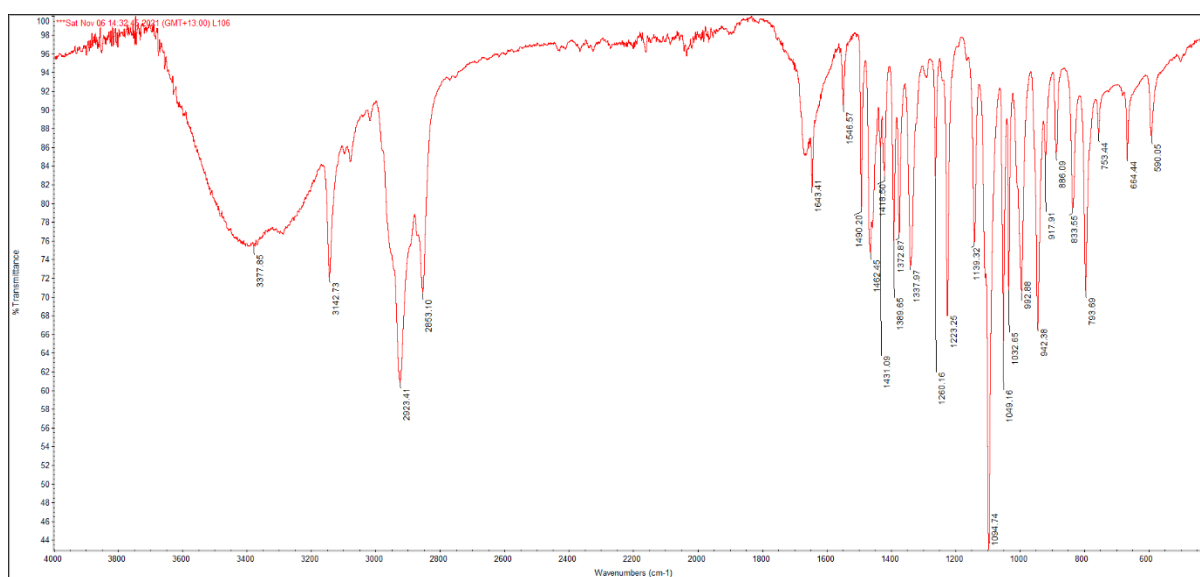


Figure S 36 ATR-IR of L1

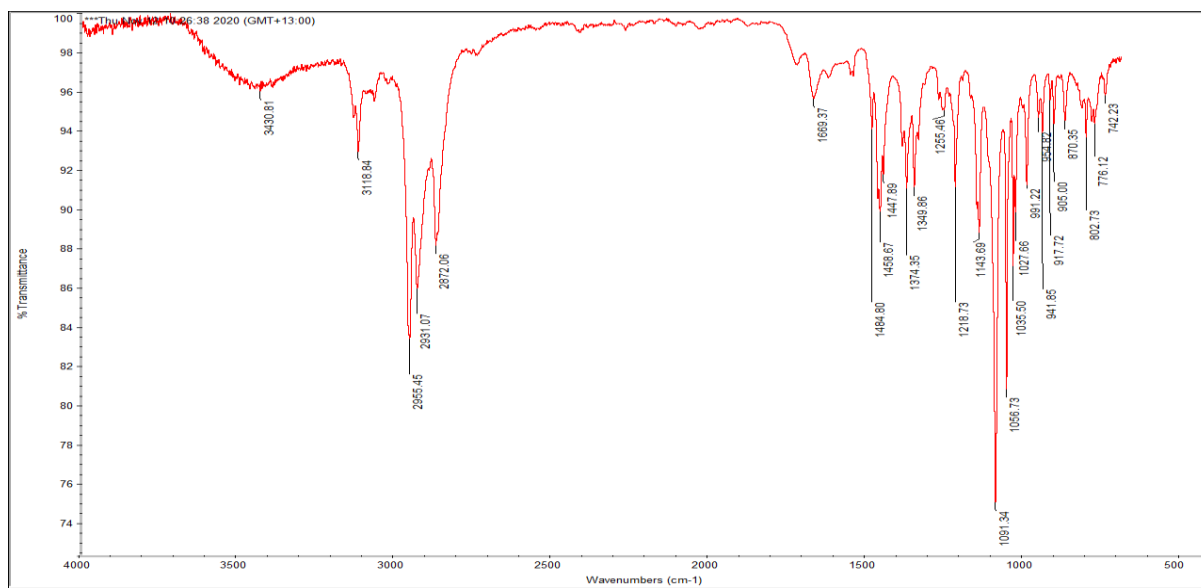


Figure S 37 ATR-IR of L2

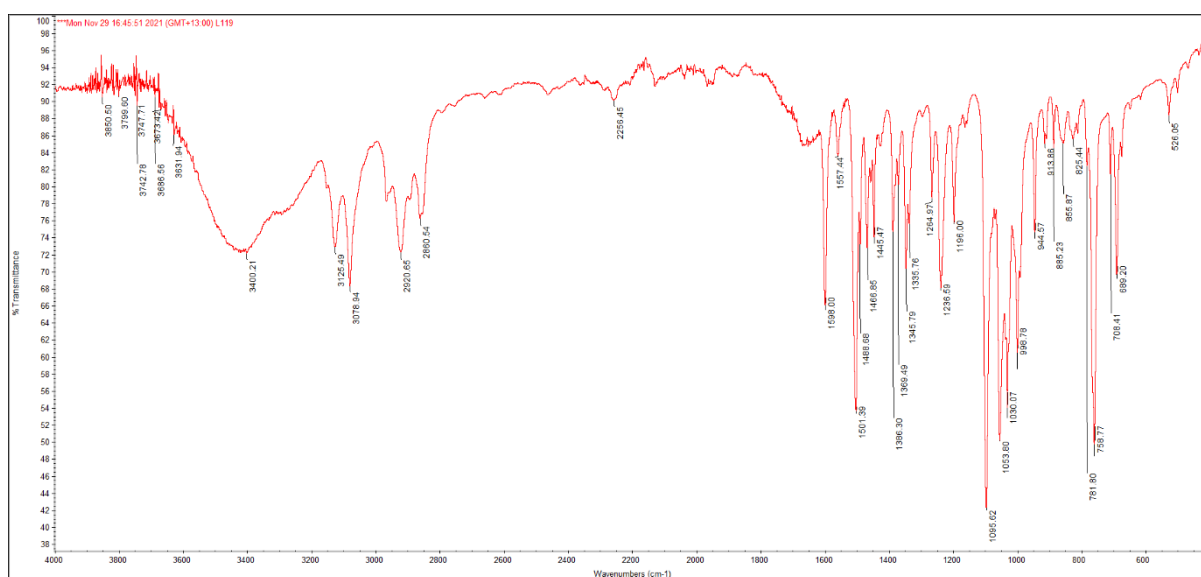


Figure S 38 ATR-IR of L3

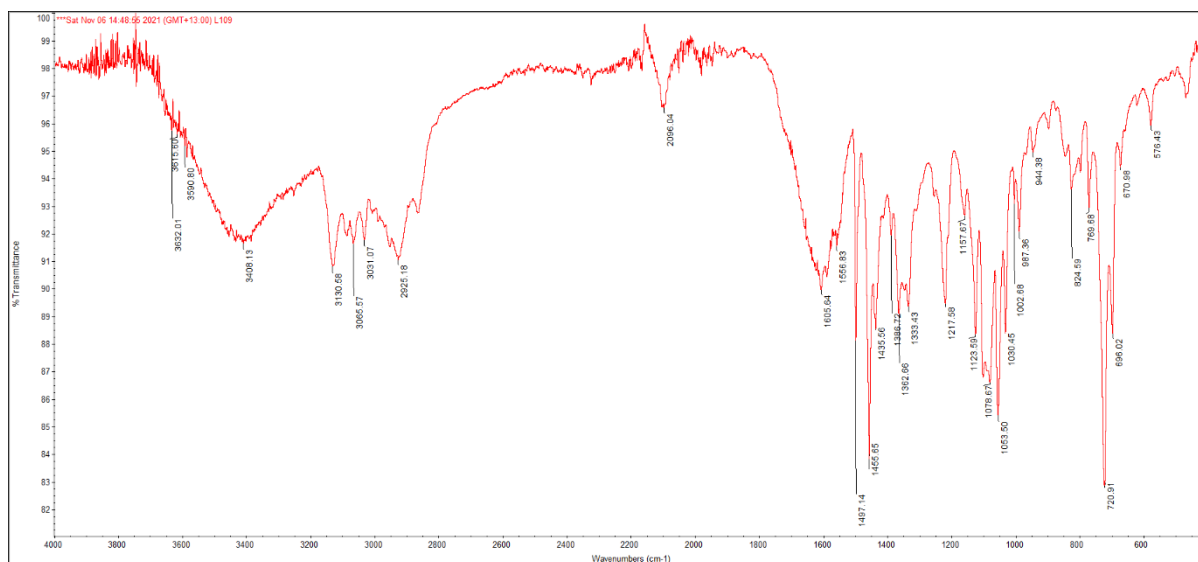


Figure S 39 ATR-IR of L4

S4.2 ATR-IR : coordination polymer complexes

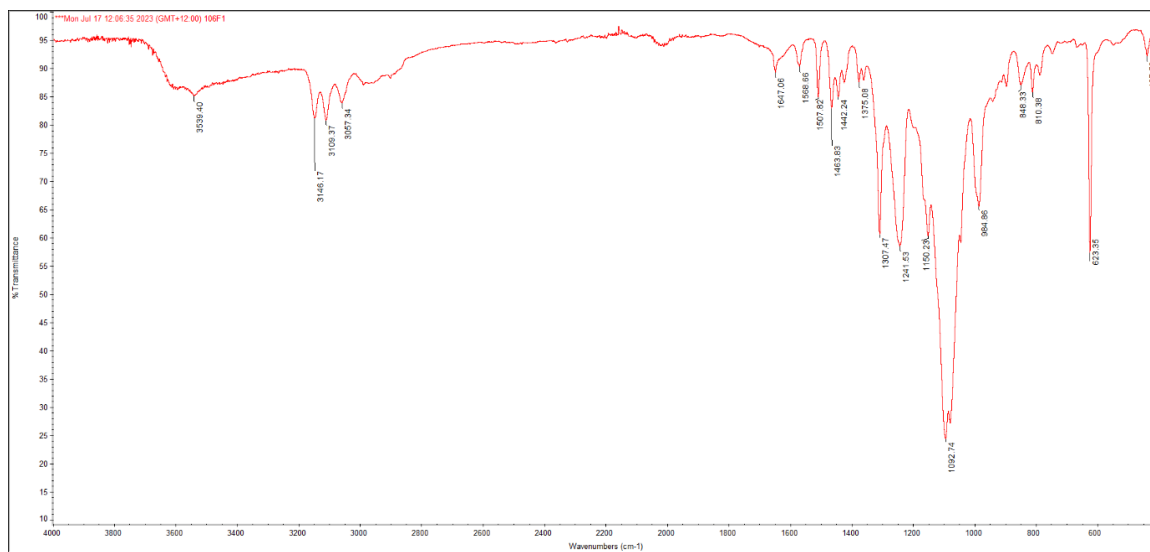


Figure S 40 Complex 1A: $\{[\text{Cu}(\text{L1})](\text{ClO}_4)_2\}_n$

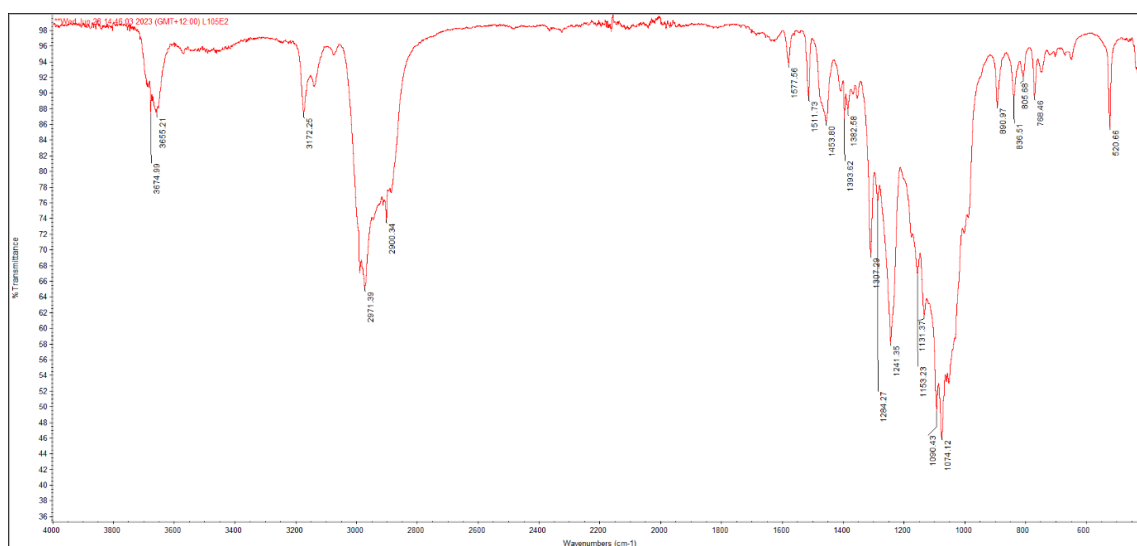


Figure S 41 Complex 2A: $\{[\text{Zn}(\text{L2})](\text{BF}_4)_2\}_n$

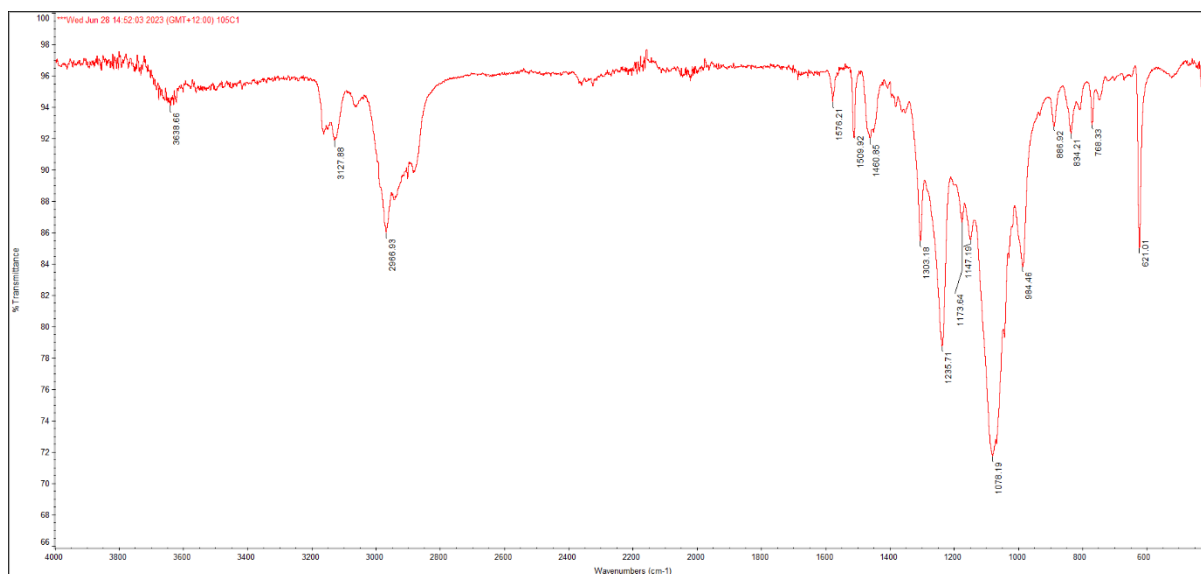


Figure S 42 Complex 2B: {[Fe(L2)](ClO4)2}n

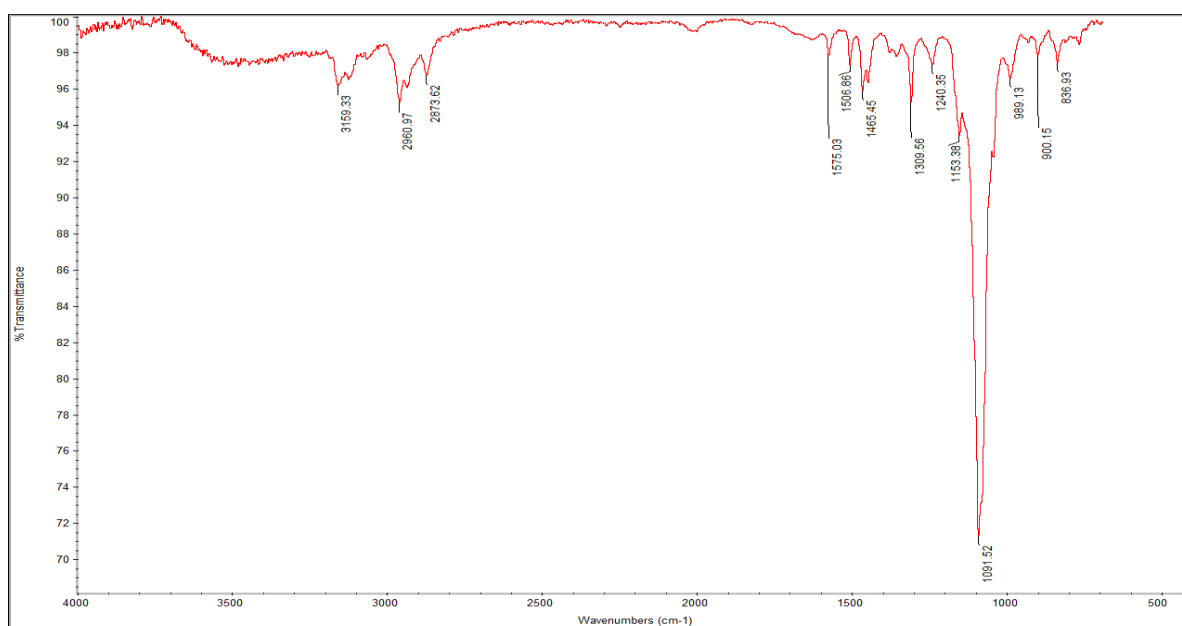


Figure S 43 Complex 2C: {[Cu(L2)](ClO4)2}n

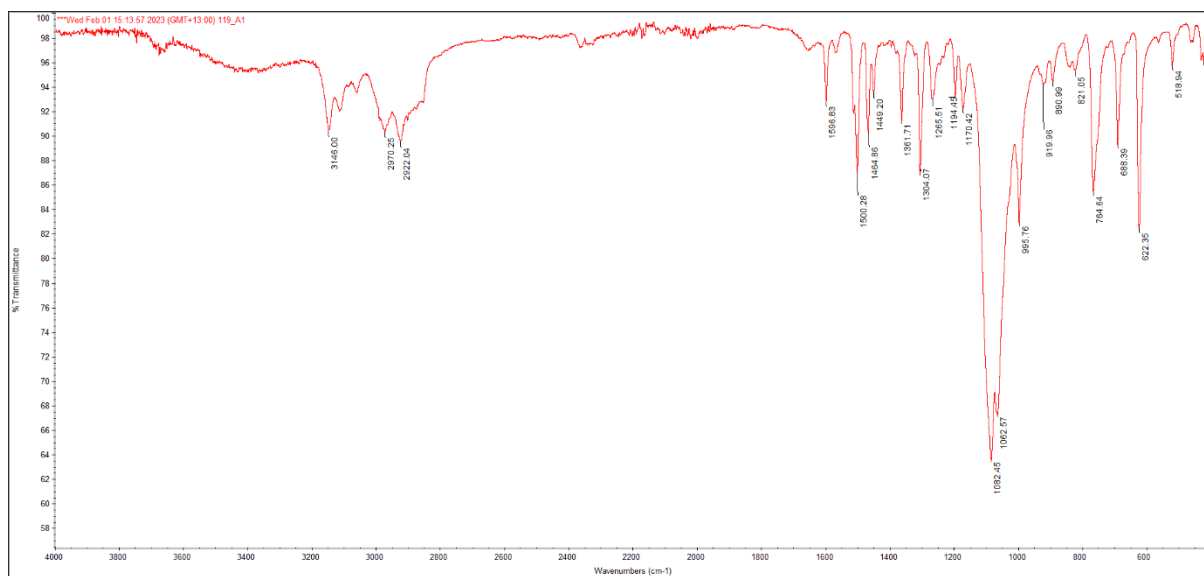


Figure S 44 Complex 3A: {[Mn(L3)](ClO4)2}n

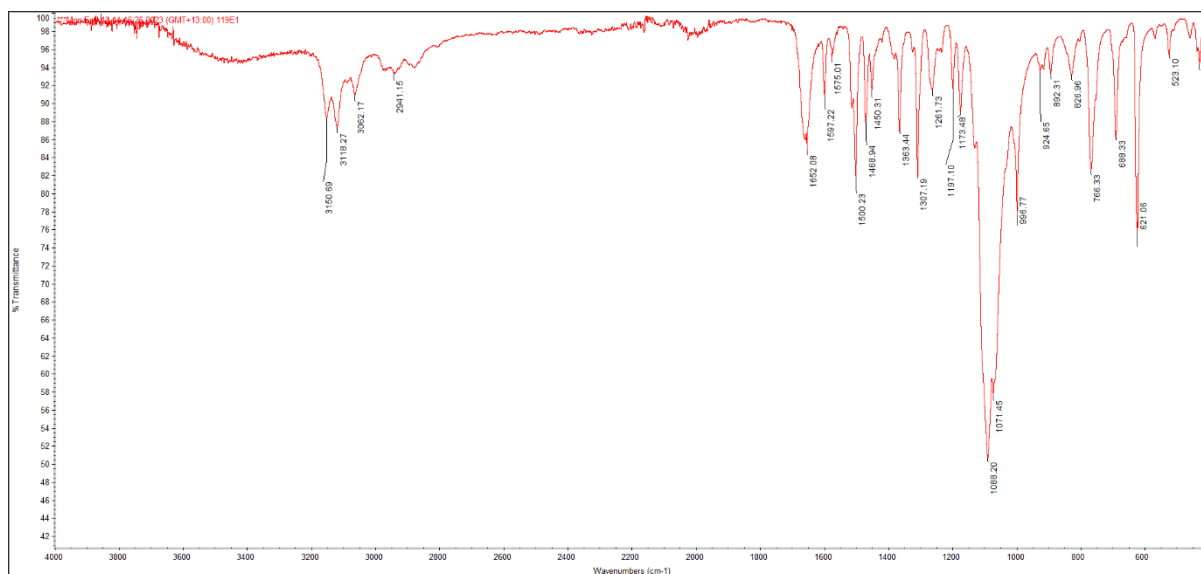


Figure S 45 Complex 3B: {[Zn(L3)](ClO4)2}

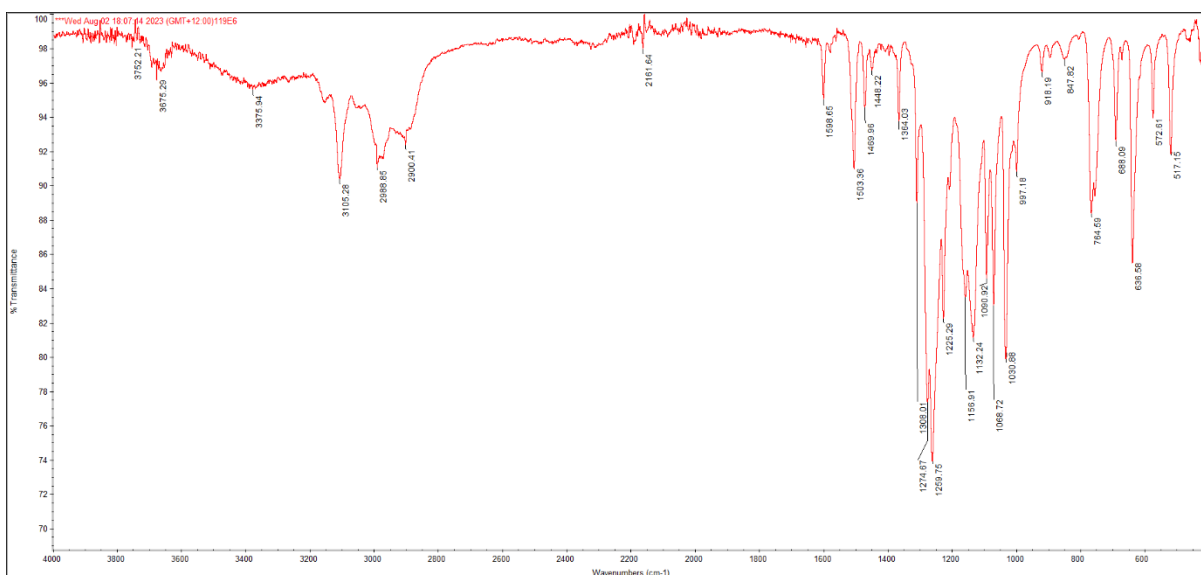


Figure S 46 3C: {[Zn(L3)](OTf)2}∞

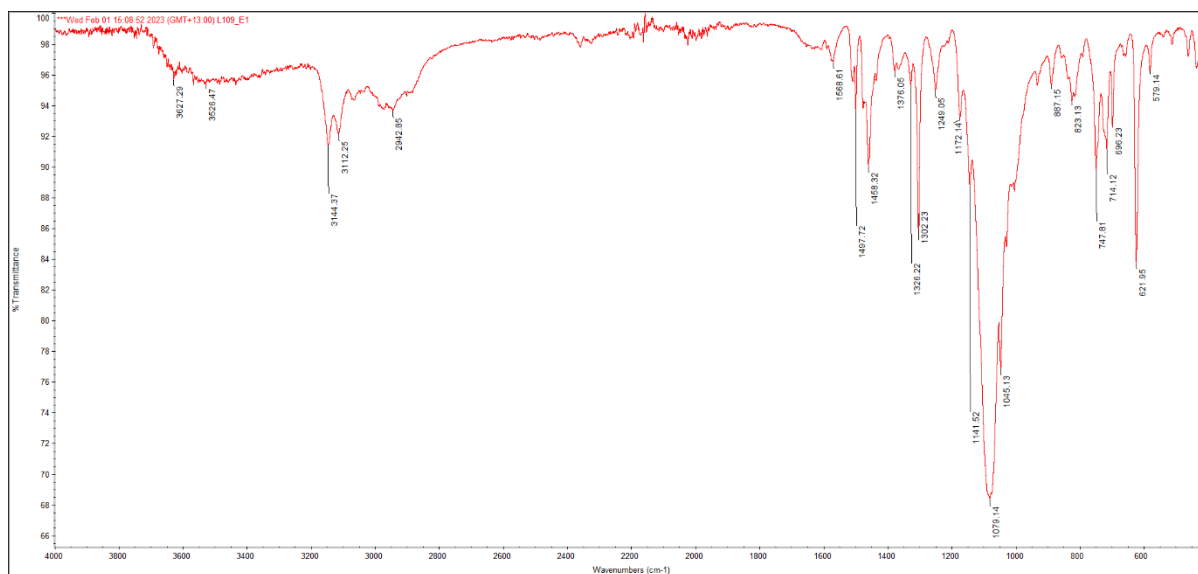


Figure S 47 Complex 4A: {[Zn(L4)](ClO4)2}n

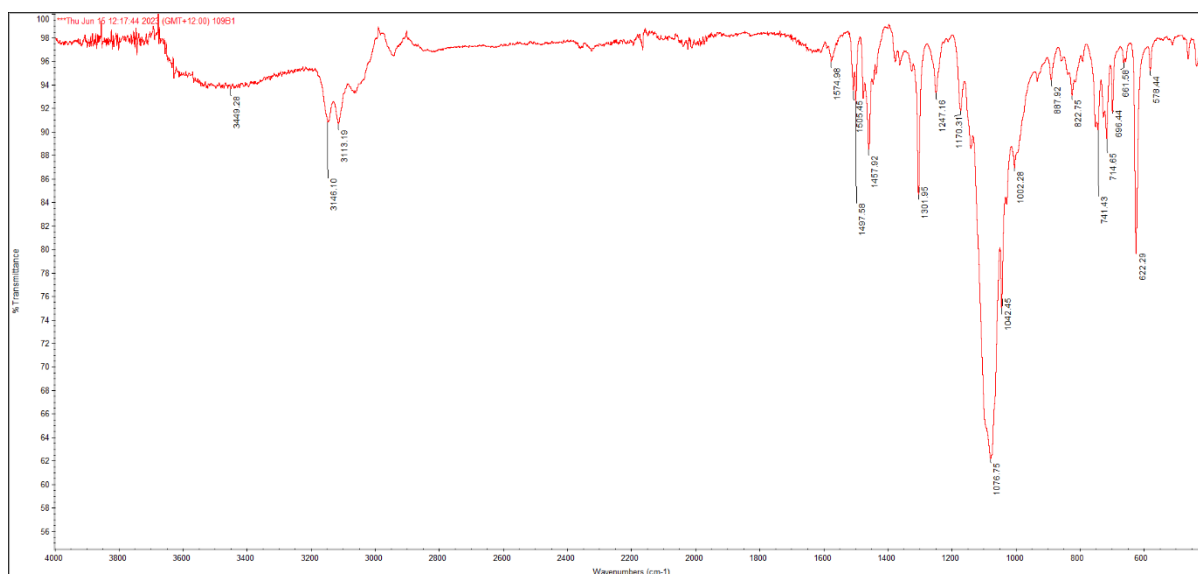


Figure S 48 Complex 4B: {[Co(L4)](ClO4)2}n

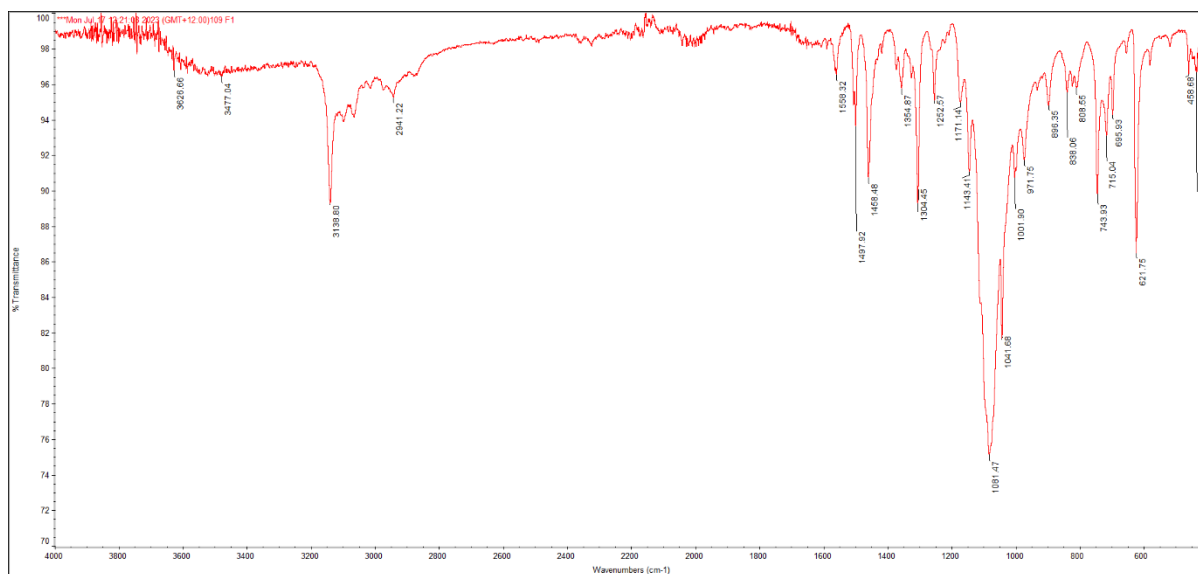


Figure S 49 Complex 4C: {[Cu(L4)](ClO4)2}n

References

1. B. Yang, H. Zhang, H. Peng, Y. Xu, B. Wu, W. Weng and L. Li, *Polym. Chem.*, 2014, **5**, 1945-1953.
2. K. Darrah, T. Wang, I. Cook, M. Cacace, A. Deiters and T. S. Leyh, *J. Biol. Chem.*, 2019, **294**, 2293-2301.
3. J.-W. Zhao, J.-W. Guo, M.-J. Huang, Y.-Z. You, Z.-H. Wu, H.-M. Liu and L.-H. Huang, *Steroids*, 2019, **150**, 108431.
4. M. Kitamura, M. Yano, N. Tashiro, S. Miyagawa, M. Sando and T. Okauchi, *Eur. J. Inorg. Chem.*, 2011, **2011**, 458-462.
5. Q. Yan, X. Shen, G. Zi and G. Hou, *Eur. J. Chem.*, 2020, **26**, 5961-5964.
6. J. Pietruszka and G. Solduga, *Eur. J. Inorg. Chem.*, 2009, **2009**, 5998-6008.
7. S. K. Das and J. Frey, *Tetrahedron Lett.*, 2012, **53**, 3869-3872.
8. D. D. Perrin, W. L. Armarego and D. R. Perrin, *Purification of laboratory chemicals*, 1988.
9. I. Delso, J. Valero-Gonzalez, F. Gomollón-Bel, J. Castro-López, W. Fang, I. Navratilova, D. M. F. van Aalten, T. Tejero, P. Merino and R. Hurtado-Guerrero, *ChemMedChem*, 2018, **13**, 128-132.